

# UV stable, Lorentz-violating dark energy with transient phantom era

Maxim Libanov and Valery Rubakov

*Institute for Nuclear Research of the Russian Academy of Sciences,  
60th October Anniversary Prospect, 7a, Moscow, 117312, Russia*

Eleftherios Papantonopoulos

*Department of Physics, National Technical University of Athens,  
Zografou Campus GR 157 73, Athens, Greece*

M. Sami

*Centre for Theoretical Physics, Jamia Millia, New Delhi-110025, India*

Shinji Tsujikawa

*Department of Physics, Gunma National College of Technology, Gunma 371-8530, Japan*

Phantom fields with negative kinetic energy are often plagued by the vacuum quantum instability in the ultraviolet region. We present a Lorentz-violating dark energy model free from this problem and show that the crossing of the cosmological constant boundary  $w = -1$  to the phantom equation of state is realized before reaching a de Sitter attractor. Another interesting feature is a peculiar time-dependence of the effective Newton's constant; the magnitude of this effect is naturally small but may be close to experimental limits. We also derive momentum scales of instabilities at which tachyons or ghosts appear in the infrared region around the present Hubble scale and clarify the conditions under which tachyonic instabilities do not spoil homogeneity of the present/future Universe.

## I. INTRODUCTION

The compilations of various observational data show that the Universe has entered the stage of an accelerated expansion around the redshift  $z \sim 1$  [1, 2, 3, 4, 5, 6]. The equation of state (EOS) parameter  $w$  of Dark Energy (DE) responsible for the acceleration of the Universe has been constrained to be close to  $w = -1$ . However, the phantom EOS ( $w < -1$ ) is still allowed by observations and even favored by some analyses of the data [7]. It is also possible that the EOS of DE crossed the cosmological constant boundary ( $w = -1$ ) in relatively near past [8].

The presence of the phantom corresponds to the violation of weak energy condition, the property which is generally difficult to accommodate within the framework of field theory. The simplest model which realizes the phantom EOS is provided by a minimally coupled scalar field with a negative kinetic term [9, 10] (see also Refs. [11, 12]). The negative kinetic energy is generally problematic because it leads to a quantum instability of the vacuum in the ultraviolet (UV) region [10, 13, 14, 15, 16, 17]: the vacuum is unstable against the catastrophic particle production of ghosts and normal (positive energy) fields.

There have been a number of attempts to realize the phantom EOS without having the pathological behaviour in the UV region. One example is scalar-tensor gravity in which a scalar field  $\phi$  with a positive kinetic term is coupled to Ricci scalar  $R$  [18, 19]. This coupling leads to the modification of gravitational constant, but it was shown in Ref. [20] that there are some parameter regions in which a phantom effective EOS is achieved without violating local gravity constraints in the present Universe.

Another example is provided by the so-called modified gravity, including  $f(R)$  gravity models [21] and the Gauss-Bonnet (GB) models [22]. In  $f(R)$  models it is possible to obtain a strongly phantom effective EOS, but in that case the preceding matter epoch is practically absent [23]. For GB DE models it was shown in Ref. [24] that the crossing of the cosmological constant boundary,  $w = -1$ , is possible, but local gravity experiments place rather strong constraints on the effective GB energy fraction [25]. In addition, tensor perturbations are typically plagued by instabilities in the UV region if the GB term is responsible for the accelerated expansion of the Universe [26]. Thus, it is generally not so easy to construct viable modified gravity models that realize the phantom effective EOS without violating cosmological and local gravity constraints.

The third example is the Dvali-Gabadadze-Porrati (DGP) braneworld model [27] and its extension [28] with a GB term in the bulk, which allow for the possibility to have  $w < -1$  [29, 30]. However, it was shown in Ref. [31] that the DGP model contains a ghost mode, which casts doubts on the viability of the self-accelerating solution.

While the above models more or less correspond to the modification of gravity, it was recently shown that in the Einstein gravity in a Lorentz-violating background the phantom EOS can be achieved without any inconsistency in the UV region [32, 33]. In particular, in the model of Ref. [33] Lorentz invariance is broken in the presence of a vector field  $B_\mu$  which has two-derivative kinetic terms similar to those given in Ref. [34]. The effect of the Lorentz violation

is quantified by a parameter  $\Xi \equiv B_\mu B^\mu / \mathcal{M}^2$ , where  $\mathcal{M}$  is an UV cut-off scale. In analogy to Ref. [35] the vector field also has one-derivative coupling  $\epsilon \partial_\mu \Phi B^\mu$  with a scalar field  $\Phi$ , where  $\epsilon$  is a small parameter that characterizes an IR scale. In the UV region, where the spatial momentum  $p$  is much larger than  $\epsilon$ , ghosts, tachyons and super-luminal modes are not present. Meanwhile tachyons or ghosts can appear in the IR region  $p \lesssim \epsilon$ . This is not problematic provided that  $\epsilon$  is close to the present Hubble scale.

In this paper we apply this Lorentz-violating model to dark energy and study the cosmological dynamics in detail in the presence of mass terms in the potential,  $V = \frac{1}{2}m^2\Phi^2 - \frac{1}{2}M^2X^2$  (where  $X = B_0$ ). We show that the model has a de Sitter attractor responsible for the late-time acceleration. At early times DE naturally has normal EOS with  $w > -1$ , while the phantom EOS can be realized between the matter-dominated era and the final de Sitter epoch. We clarify the conditions under which the cosmological constant boundary crossing to the phantom region occurs. Interestingly, in a range of parameters this crossing takes place at the epoch when  $\Omega_m \sim \Omega_{\text{DE}}$  thus making the crossing potentially observable.

An interesting feature of our model is the time-dependence of the effective Newton's constant. It is naturally weak, but may well be comparable with current experimental limits. Moreover, the effective Newton's constant  $G_*(t)$  has a peculiar behaviour correlated with the deviation of  $w$  from  $-1$ .

We also derive momentum scales of instabilities of perturbations, first in Minkowski spacetime. This is the extension of the work [33] that mainly focused on the case of massless scalar ( $m = 0$ ). We show that in the UV region ( $p \gg \epsilon$ ) the model does not have any unhealthy states such as ghosts, tachyons or super-luminal modes. In the IR region ( $p \lesssim \epsilon$ ) tachyons or ghosts appear, depending on the momentum. Finally, we study the evolution of perturbations in the cosmological background and estimate the amplitude of perturbations amplified by the tachyonic instability around the scale of the present Hubble radius. The perturbations remain to be smaller than the background fields under certain restriction on the model parameters.

This paper is organized as follows. In Sec. II we present our Lorentz-violating model and derive basic equations describing spatially flat Friedmann-Robertson-Walker cosmology in the presence of DE, radiation and non-relativistic matter. In Sec. III we derive the fixed points of the system by rewriting the equations in autonomous form. The cosmological dynamics is discussed in detail analytically and numerically with an emphasis on the occurrence of a phantom phase before reaching a de Sitter attractor. The time-dependence of the effective gravitational constant is also considered. In Sec. IV we study the Minkowski spectrum of field perturbations and clarify the properties of tachyons and ghosts in the IR region. We then discuss the tachyonic amplification of field perturbations around the present Hubble scale in the cosmological background. We summarize our results in Sec. V.

## II. LORENTZ-VIOLATING MODEL

We study a 4-dimensional Lorentz-violating model whose Lagrangian density includes a vector field  $B_\mu$  and a scalar field  $\Phi$ :

$$\mathcal{L} = -\frac{1}{2}\alpha(\Xi)g^{\nu\lambda}D_\nu B_\nu D^\mu B_\lambda + \frac{1}{2}\beta(\Xi)D_\mu B_\nu D^\mu B_\lambda \frac{B^\nu B^\lambda}{\mathcal{M}^2} + \frac{1}{2}\partial_\mu \Phi \partial^\mu \Phi + \epsilon \partial_\mu \Phi B^\mu - V(B, \Phi), \quad (1)$$

where  $\Xi = B_\mu B^\mu / \mathcal{M}^2$  with  $\mathcal{M}$  being an UV cut-off scale of the effective theory. The dimensionless parameters  $\alpha$  and  $\beta$  are the functions of  $\Xi$ , and  $\epsilon$  is a free positive parameter that characterizes an IR scale. The first two terms in (1) are familiar in two-derivative theory [34], whereas the one-derivative term  $\epsilon \partial_\mu \Phi B^\mu$  is introduced following the approach of Ref. [35].

We study dynamics of flat Friedmann-Robertson-Walker (FRW) Universe

$$ds^2 = \mathcal{N}^2(t)dt^2 - a^2(t)d\mathbf{x}^2, \quad (2)$$

where  $\mathcal{N}(t)$  is a Lapse function and  $a(t)$  is a scale factor. In the case of spatially homogeneous fields with  $B_i = 0$  ( $i = 1, 2, 3$ ), the Lagrangian (1) reads

$$\sqrt{-g}\mathcal{L} = \frac{\gamma a^3}{2\mathcal{N}}\dot{X}^2 - \frac{3\alpha \dot{a}^2 a}{2\mathcal{N}}X^2 + \frac{1}{2}\frac{a^3}{\mathcal{N}}\dot{\phi}^2 + \epsilon a^3 \dot{\phi}X - a^3 \mathcal{N}V(X, \phi), \quad (3)$$

where  $X = B_0/\mathcal{N}$ ,  $\phi$  is the homogeneous part of the field  $\Phi$  and

$$\gamma(X) = \frac{X^2}{\mathcal{M}^2}\beta(X) - \alpha(X). \quad (4)$$

Hereafter we study the case in which the following condition holds

$$\alpha > \gamma > 0.$$

This is required to avoid a superluminal propagation in Minkowski spacetime [33], as we will see later. Throughout this paper we assume that  $\alpha$  and  $\gamma$  are of order unity.

The second term in the Lagrangian (3) leads to the change of the ‘‘cosmological’’ effective Planck mass [33]

$$m_{\text{pl,cosm}}^2 = m_{\text{pl}}^2 + 4\pi\alpha X^2. \quad (5)$$

Another effective Planck mass  $m_{\text{pl,Newton}}$  determines the strength of gravitational interactions at distances much shorter than the cosmological scale; in general, these two effective Planck masses are different [19, 35, 36]. We show in Appendix A that the ‘‘Newtonian’’ Planck mass in our model is given by

$$m_{\text{pl,Newton}}^2 = m_{\text{pl}}^2 - 4\pi\alpha X^2. \quad (6)$$

Both effective Planck masses depend on time via  $X = X(t)$ . Since the time-dependent terms in (5) and (6) differ by sign only, it will be sufficient to study one of these effective masses. In what follows we concentrate on the ‘‘Newtonian’’ mass (6) for definiteness.

In this paper we focus on the case in which the potential  $V$  is written in a separable form:

$$V = W(\phi) + U(X). \quad (7)$$

We take into account the contributions of non-relativistic matter and radiation whose energy densities  $\rho_m$  and  $\rho_r$ , respectively, satisfy

$$\dot{\rho}_m + 3H\rho_m = 0, \quad (8)$$

$$\dot{\rho}_r + 4H\rho_r = 0. \quad (9)$$

The energy density of the fields is derived by taking the derivative with respect to  $\mathcal{N}$  of the action  $S = \int d^4x \sqrt{-g} \mathcal{L}$ :

$$\rho = -\frac{1}{a^3} \left[ \frac{\delta S}{\delta \mathcal{N}} \right]_{\mathcal{N}=1} = \frac{\gamma}{2} \dot{X}^2 - \frac{3\alpha}{2} H^2 X^2 + \frac{1}{2} \dot{\phi}^2 + V. \quad (10)$$

We set  $\mathcal{N} = 1$  for the rest of this paper.

The Friedmann equation is given by

$$H^2 \equiv \left( \frac{\dot{a}}{a} \right)^2 = \frac{\kappa^2}{3} \left[ \frac{1}{2} \gamma \dot{X}^2 - \frac{3\alpha}{2} H^2 X^2 + \frac{1}{2} \dot{\phi}^2 + W(\phi) + U(X) + \rho_m + \rho_r \right], \quad (11)$$

where  $\kappa^2 = 8\pi/m_{\text{pl}}^2$ . The equations of motion for the homogeneous fields  $\phi$  and  $\chi$  are

$$-\gamma \left( \ddot{X} + 3H\dot{X} \right) - \frac{1}{2} \gamma_{,X} \dot{X}^2 - \frac{3}{2} \alpha_{,X} H^2 X^2 - 3\alpha H^2 X + \epsilon \dot{\phi} = U_{,X}, \quad (12)$$

$$-(\ddot{\phi} + 3H\dot{\phi}) - \epsilon(\dot{X} + 3HX) = W_{,\phi}, \quad (13)$$

where  $\gamma_{,X} = d\gamma/dX$ , etc. Taking the time-derivative of Eq. (11) and using Eqs. (12) and (13), we obtain

$$\dot{H} = -\frac{\kappa^2}{2} \left( \rho + p + \rho_m + \frac{4}{3} \rho_r \right),$$

where

$$\rho + p = \epsilon \dot{\phi} X + \alpha \dot{H} X^2 + 2\alpha H X \dot{X} + \gamma \dot{X}^2 + \dot{\phi}^2 + \alpha_{,X} H X^2 \dot{X}. \quad (14)$$

In what follows we assume for simplicity that  $\alpha$  and  $\gamma$  are constants, i.e.,  $\alpha_{,X} = \gamma_{,X} = 0$ .

Following Ref. [33] we consider the simplest potential for the fields,

$$W(\phi) = \frac{1}{2} m^2 \phi^2, \quad U(X) = -\frac{1}{2} M^2 X^2, \quad (15)$$

which allows for a possibility to realize a phantom phase.

One immediate point to note is that in the absence of radiation and matter, the system of equations (11), (12), (13) has a de Sitter solution,  $H = \text{const}$ , for which  $\phi$  and  $X$  are also independent of time, provided that

$$\frac{\epsilon}{m} > \sqrt{\frac{2\alpha}{3}}. \quad (16)$$

Indeed, for constant  $H, \phi$  and  $X$  eqs. (11), (12), (13) reduce to a simple algebraic system

$$\begin{aligned} H^2 &= \frac{\kappa^2}{3} \left[ -\frac{3\alpha}{2} H^2 X^2 - \frac{M^2}{2} X^2 + \frac{m^2}{2} \phi^2 \right], \\ 3\alpha H^2 &= M^2, \\ -3\epsilon H X &= m^2 \phi. \end{aligned} \quad (17)$$

Once the inequality (16) is satisfied, this system has a solution

$$\begin{aligned} H_A &= \frac{M}{\sqrt{3\alpha}}, \\ \phi_A &= \sqrt{\frac{3}{4\pi}} \frac{M m_{\text{pl}} \epsilon}{\sqrt{\alpha m^2}} \frac{1}{\sqrt{3\epsilon^2/m^2 - 2\alpha}}, \\ X_A &= -\frac{m_{\text{pl}}}{\sqrt{4\pi}} \frac{1}{\sqrt{3\epsilon^2/m^2 - 2\alpha}}. \end{aligned} \quad (18)$$

We will see in Secs. III and IV that in a range of parameters this solution is an attractor which corresponds to the de Sitter phase in asymptotic future. In order to use this for dark energy we require that the mass scale  $M$  is the order of the present Hubble parameter  $H_0$ . Then the Newtonian effective Planck mass, Eq. (6), is given by

$$m_{\text{pl,Newton}}^2 = m_{\text{pl}}^2 \left( 1 - \frac{\alpha}{3\epsilon^2/m^2 - 2\alpha} \right). \quad (19)$$

In order that the change of the Planck mass be small, we impose the condition

$$\epsilon \gg \sqrt{\alpha} m. \quad (20)$$

Another point to note is that at early times, when the Hubble parameter is large enough, the term  $(-3\alpha H^2 X)$  in Eq. (12) drives the field  $X$  to zero, the relevant time being of the order of the Hubble time. Soon after that the field  $\phi$  obeys the usual scalar field equation in expanding Universe, the Hubble friction freezes this field out. Thus, the initial data for the interesting part of the DE evolution are

$$\begin{aligned} X_i &= 0, \\ \phi_i &= \text{const}. \end{aligned} \quad (21)$$

The value of  $\phi_i$  is a free parameter of the cosmological evolution in our model. Clearly, EOS for DE at early times is normal,  $w > -1$ , with  $w$  being close to  $-1$ . We find in Sec. III that before reaching the de Sitter asymptotics (18) the system may pass through a transient phantom phase with  $w < -1$ .

### III. DYNAMICS OF DARK ENERGY

We are going to study whether our model can lead to the sequence of radiation, matter and accelerated epochs. Moreover, we wish to clarify the conditions under which the system behaves as a phantom before reaching the accelerated attractor (18). In this section we analyze the cosmological dynamics by using autonomous equations, the techniques widely used in the context of dark energy studies [6, 38, 39].

#### A. Autonomous equations

Let us define the following dimensionless variables which are convenient for studying the dynamical system [6, 38]:

$$x_1 = \frac{\kappa\sqrt{\gamma}\dot{X}}{\sqrt{6}H}, \quad x_2 = \frac{\kappa\dot{\phi}}{\sqrt{6}H}, \quad x_3 = \frac{\kappa m\phi}{\sqrt{6}H}, \quad x_4 = \sqrt{\frac{4\pi}{3}} \frac{X}{m_{\text{pl}}}, \quad x_5 = \frac{M}{H}, \quad x_6 = \frac{\kappa\sqrt{\rho_r}}{\sqrt{3}H}. \quad (22)$$

Then we obtain the following autonomous equations

$$x'_1 = -3x_1 - \frac{3\alpha}{\sqrt{\gamma}} x_4 + \frac{\epsilon}{M} \frac{1}{\sqrt{\gamma}} x_2 x_5 + \frac{1}{\sqrt{\gamma}} x_4 x_5^2 - x_1 \frac{H'}{H}, \quad (23)$$

$$x'_2 = -3x_2 - \frac{\epsilon}{M} \frac{1}{\sqrt{\gamma}} x_1 x_5 - 3 \frac{\epsilon}{M} x_4 x_5 - \frac{m}{M} x_3 x_5 - x_2 \frac{H'}{H}, \quad (24)$$

$$x'_3 = \frac{m}{M} x_2 x_5 - x_3 \frac{H'}{H}, \quad (25)$$

$$x'_4 = \frac{1}{\sqrt{\gamma}} x_1, \quad (26)$$

$$x'_5 = -x_5 \frac{H'}{H}, \quad (27)$$

$$x'_6 = -2x_6 - x_6 \frac{H'}{H}, \quad (28)$$

and

$$\frac{H'}{H} = -\frac{3}{2} \frac{1 + x_1^2 + x_2^2 - x_3^2 + x_4^2(3\alpha + x_5^2) + x_6^2/3 + 2(\epsilon/M)x_2x_4x_5 + 4(\alpha/\sqrt{\gamma})x_1x_4}{1 + 3\alpha x_4^2},$$

where prime denotes the derivative with respect to

$$N \equiv \ln(a).$$

Equation (11) gives the constraint

$$\Omega_m \equiv \frac{\kappa^2 \rho_m}{3H^2} = 1 - x_1^2 - x_2^2 - x_3^2 + x_4^2(3\alpha + x_5^2) - x_6^2. \quad (29)$$

We also define the following quantities

$$\Omega_r \equiv \frac{\kappa^2 \rho_r}{3H^2} = x_6^2, \quad (30)$$

$$\Omega_{\text{DE}} \equiv 1 - \Omega_m - \Omega_r = x_1^2 + x_2^2 + x_3^2 - x_4^2(3\alpha + x_5^2).$$

The effective EOS parameter of the entire system is given by

$$w_{\text{eff}} = -1 - \frac{2}{3} \frac{H'}{H}.$$

Meanwhile the EOS parameter of DE is

$$w = \frac{p}{\rho} = \frac{w_{\text{eff}} - \Omega_r/3}{1 - \Omega_m - \Omega_r}. \quad (31)$$

Note that the above equations are invariant under the simultaneous change of the signs of  $\phi$  and  $X$ . Hence it is not restrictive to study the case of positive  $\phi$ . Note also that we study the case of an expanding Universe with  $H > 0$ .

## B. Fixed points

By setting  $x'_i = 0$  one formally finds the following six fixed points:

- (A) de Sitter (i):  $(x_1, x_2, x_3, x_4, x_5, x_6) = \left(0, 0, \frac{\epsilon}{m} \sqrt{\frac{3}{3\epsilon^2/m^2 - 2\alpha}}, -\frac{1}{\sqrt{3(3\epsilon^2/m^2 - 2\alpha)}}, \sqrt{3\alpha}, 0\right),$
- (B) de Sitter (ii):  $(x_1, x_2, x_3, x_4, x_5, x_6) = (0, 0, \text{const}, 0, 0, 0),$
- (C) matter:  $(x_1, x_2, x_3, x_4, x_5, x_6) = (0, 0, 0, 0, 0, 0),$
- (D) radiation:  $(x_1, x_2, x_3, x_4, x_5, x_6) = (0, 0, 0, 0, 0, 1),$
- (E1) kinetic point (i):  $(x_1, x_2, x_3, x_4, x_5, x_6) = (0, 1, 0, 0, 0, 0),$
- (E2) kinetic point (ii):  $(x_1, x_2, x_3, x_4, x_5, x_6) = (0, -1, 0, 0, 0, 0).$

The fixed point (A) is precisely the de Sitter solution (18) that we discussed in Sec. II. We will comment on its stability shortly.

The point (B) is also in some sense a de Sitter point. It exists even in the absence of the field  $X$  and satisfies the relation  $3H^2 = \kappa^2 W(\phi)$ . To reach the solution (B), the Hubble parameter needs to increase towards infinity ( $M/H \rightarrow 0$ ), and the field  $\phi$  needs to diverge as well.

The point (C) corresponds to matter-dominated era satisfying  $\Omega_m = 1$  and  $w_{\text{eff}} = 0$ , whereas the point (D) describes radiation-dominated epoch with  $\Omega_r = 1$  and  $w_{\text{eff}} = 1/3$ .

The points (E1) and (E2) are kinetic solutions satisfying  $\Omega_{\text{DE}} = 1$  and  $w_{\text{eff}} = 1$ . These solutions are used neither for dark energy nor for radiation/matter dominated epochs.

A cosmologically viable trajectory starts from the radiation point (D), connects to the matter solution (C) and finally approaches the de Sitter point (A). [Note that the initial data (21) indeed correspond to  $x_1, x_2, x_3, x_4, x_5 \rightarrow 0$  as  $t \rightarrow 0$ .] In Appendix B we show that this sequence is indeed possible by studying the stability of fixed points against perturbations. In particular, the stability of the de Sitter point (A) is important for having the late-time accelerated epoch. This depends upon the two ratios  $\epsilon/m$  and  $M/m$  once the parameters  $\alpha$  and  $\gamma$  are fixed. When  $\alpha = 1$  and  $\gamma = 1/2$ , for example, the parameter range of  $\epsilon/m$  is determined by the ratio  $M/m$ . We find that the point (A) is a stable attractor if the following conditions hold:

- (i) When  $M/m = 0.1$ ,  $\epsilon/m > 0.817$ ,
- (ii) When  $M/m = 1$ ,  $\epsilon/m > 1.35$ ,
- (iii) When  $M/m = 10$ ,  $\epsilon/m > 3.52$ ,

When  $\epsilon \gg m$ , the stability of the point (A) is ensured automatically unless the ratio  $M/m$  is too much larger than unity. In view of (20) the case  $\epsilon \gg m$  is of particular interest.

If the condition  $\epsilon \gg M$  is also satisfied, it is possible that the solutions pass through a phantom region and then approach the de Sitter attractor (A). In the next subsection we discuss the phantom phase during which the dark energy equation of state  $w$  becomes smaller than  $-1$ .

### C. Phantom solutions

Before reaching the de Sitter solution (A), the system may pass through a phantom region with  $w < -1$ . This is the stage in which the  $\epsilon$ -dependent terms are important in Eqs. (12) and (13). To see what happens, we truncate Eqs. (12) and (13) to

$$\epsilon \dot{\phi} - 3\alpha H^2 X = U_{,X}, \quad (32)$$

$$-3\epsilon H X = W_{,\phi}. \quad (33)$$

This truncation is legitimate provided that in addition to the usual slow-roll conditions  $\ddot{\phi} \ll H\dot{\phi}$  and  $\ddot{X} \ll H\dot{X}$ , the following conditions are satisfied:

$$\dot{X} \ll HX, \quad (34)$$

$$\dot{\phi} \ll \epsilon X, \quad (35)$$

$$\epsilon \dot{\phi} X \ll V. \quad (36)$$

When writing inequalities, we always mean the absolute values of the quantities. Note that we do not impose the condition  $\epsilon \dot{\phi} \gg 3\alpha H^2 X$  unlike in Ref. [33], since the term  $3\alpha H^2 X$  is not necessarily negligible relative to the term  $\epsilon \dot{\phi}$  in Eq. (32).

From Eq. (32) we obtain

$$X = \epsilon \dot{\phi} / (3\alpha H^2 - M^2).$$

Substituting this into Eq. (33) we get the following equation

$$3H\dot{\sigma} = \xi W_{,\sigma}, \quad (37)$$

where

$$\begin{aligned}\sigma &\equiv \frac{\epsilon}{M}\phi, \\ \xi &\equiv 1 - 3\alpha\frac{H^2}{M^2}, \\ W(\sigma) &\equiv \frac{m^2M^2}{2\epsilon^2}\sigma^2.\end{aligned}\tag{38}$$

This shows that the field  $\sigma$  rolls *up* the potential for  $\xi > 0$ , i.e., for

$$H < \frac{M}{\sqrt{3\alpha}}.\tag{39}$$

This is the region in which the phantom equation of state ( $w < -1$ ) can be realized. Note that Eq. (14) gives  $\rho + p \approx \epsilon\dot{\phi}X = \xi XU_{,X}$ . When  $X < 0$  we have  $w < -1$  for  $U_{,X} > 0$ , which is the case for our model (15). From Eqs. (32) and (35) we get the following condition

$$\epsilon^2 \gg \xi M^2.\tag{40}$$

In the regime in which the phantom phase ends up in the stable late-time de Sitter solution, the Hubble parameter reaches a minimum  $H_{\min} < M/\sqrt{3\alpha}$  and then increases towards the de Sitter attractor characterized by  $H = M/\sqrt{3\alpha}$ . The effective EOS parameter  $w_{\text{eff}}$  becomes smaller than  $-1$  when  $H$  begins to grow, whereas the crossing of  $w = -1$  by DE occurs earlier than that. For smaller  $H_{\min}$  the minimum values of  $w$  and  $w_{\text{eff}}$  deviate from  $-1$  more significantly. The latter cases correspond to  $\alpha H^2 \ll M^2$  (as studied in Ref. [33]), giving  $\xi \simeq 1$  from Eq. (38). In what follows we study a moderate case in which  $\alpha H^2$  is not much smaller than  $M^2$ ; in other words  $\xi$  is not much smaller than 1, say,  $\xi = \mathcal{O}(0.1)$ .

Taking the time derivative of Eq. (33) gives the relation  $\dot{X} \sim m^2 M^2 \xi X / (3H\epsilon^2)$ , where we assume that the term  $(-3\alpha H^2 X)$  does not dominate in Eq. (32). Substituting this into Eq. (34) and using Eq. (33), we find

$$3\xi U \ll W.\tag{41}$$

This shows that the potential  $W$  dominates in the Friedmann equation, so that

$$3H^2 = \kappa^2 W.\tag{42}$$

Making use of Eqs. (32) and (41), the condition (36) translates into

$$\dot{\sigma}^2 \ll \xi W.$$

From Eq. (37) this can be written as

$$\varepsilon_s \equiv \frac{1}{3\kappa^2} \left( \frac{W_{,\sigma}}{W} \right)^2 \xi = \frac{M^2 m_{\text{pl}}^2}{6\pi\epsilon^2 \phi^2} \xi \ll 1,\tag{43}$$

where  $\varepsilon_s$  can be regarded as a slow-roll parameter for the field  $\sigma$ . Since the Hubble parameter during the phantom phase is bounded from above ( $H < M/\sqrt{3\alpha}$ ), this gives the upper bound on the field  $\phi$ . By using Eq. (42) together with Eq. (43) one finds that the field  $\phi$  during the phantom phase is constrained to be in the region

$$\frac{M m_{\text{pl}} \sqrt{\xi}}{\sqrt{6\pi\epsilon}} \ll \phi < \frac{1}{\sqrt{4\pi}} \frac{M m_{\text{pl}}}{\sqrt{\alpha m}},\tag{44}$$

which requires

$$\epsilon \gg \sqrt{\alpha\xi} m.\tag{45}$$

This is similar to the condition (20).

From Eqs. (39), (41) and (42) we find that the field  $X$  satisfies the following relation during the phantom epoch

$$\alpha X^2 \ll \frac{m_{\text{pl}}^2}{12\pi\xi}.\tag{46}$$

Hence the deviation from the bare Planck mass during the phantom epoch is small indeed. In the next section, among other things, we numerically calculate the variation of the effective gravitational constant  $G_* = 1/m_{\text{pl,Newton}}^2$  before and around the present epoch.

### D. Cosmological dynamics

In this section we study numerically cosmological dynamics in our Lorentz-violating model. As we already discussed, both radiation and matter fixed points satisfy  $x_1 = x_2 = x_3 = x_4 = x_5 = 0$ . This means that the contribution of the energy density of the fields  $\phi$  and  $X$  is negligible during these epochs. The initial radiation era is followed by a matter saddle point (C). In our numerical analysis we choose initial conditions  $x_1 = x_2 = x_4 = 0$  (that is  $\dot{X} = \dot{\phi} = X = 0$ ) with nonzero values of  $x_3$ ,  $x_5$ , and  $x_6$  (that is  $\phi$ ,  $\rho_m$  and  $\rho_r$ ). This choice corresponds to the initial data (21). We have also tried many other initial conditions and found that the results are not sensitive to the initial values of  $X$ ,  $\dot{X}$  and  $\dot{\phi}$ , in accord with the discussion in the end of Sec. II.

The variable  $x_5 = M/H$  increases with the decrease of  $H$  during radiation and matter epochs. Unless the Hubble parameter begins to grow from some time onward, the solutions do not approach the de Sitter point (B) with  $x_5 = 0$  but approach the de Sitter point (A) with  $x_5 = \sqrt{3\alpha}$ . The increase of  $H$  can be realized during the phantom stage we discussed in the previous section. However, this stage occurs in the finite region of the field  $\phi$  given in Eq. (44), whereas the point (B) corresponds to the divergent field ( $\phi \rightarrow \infty$ ). Hence the solutions approach finally the de Sitter point (A) rather than (B).

In Fig. 1 we plot the cosmological evolution for the model parameters  $\alpha = 1$ ,  $\gamma = 1/2$ ,  $\epsilon/m = 3$  and  $M/m = 1$ . The left panel clearly shows that the sequence of radiation, matter and de Sitter epochs can be achieved together with the  $w = -1$  crossing. The DE EOS parameter  $w$  is nearly a constant,  $w \simeq -1$ , during the radiation and matter epochs because the fields are almost frozen. After the matter era,  $w$  begins to grow because the kinetic energies of the fields become important. However, the system soon enters the phantom phase during which the field  $\phi$  rolls up the potential. Hence the equation of state  $w$  crosses the cosmological constant boundary  $w = -1$  and reaches a minimum value  $w_{\min} < -1$ . The solution finally approaches the de Sitter point (A) with  $x_5 = \sqrt{3\alpha}$  from the phantom side (see the left panel of Fig. 1).

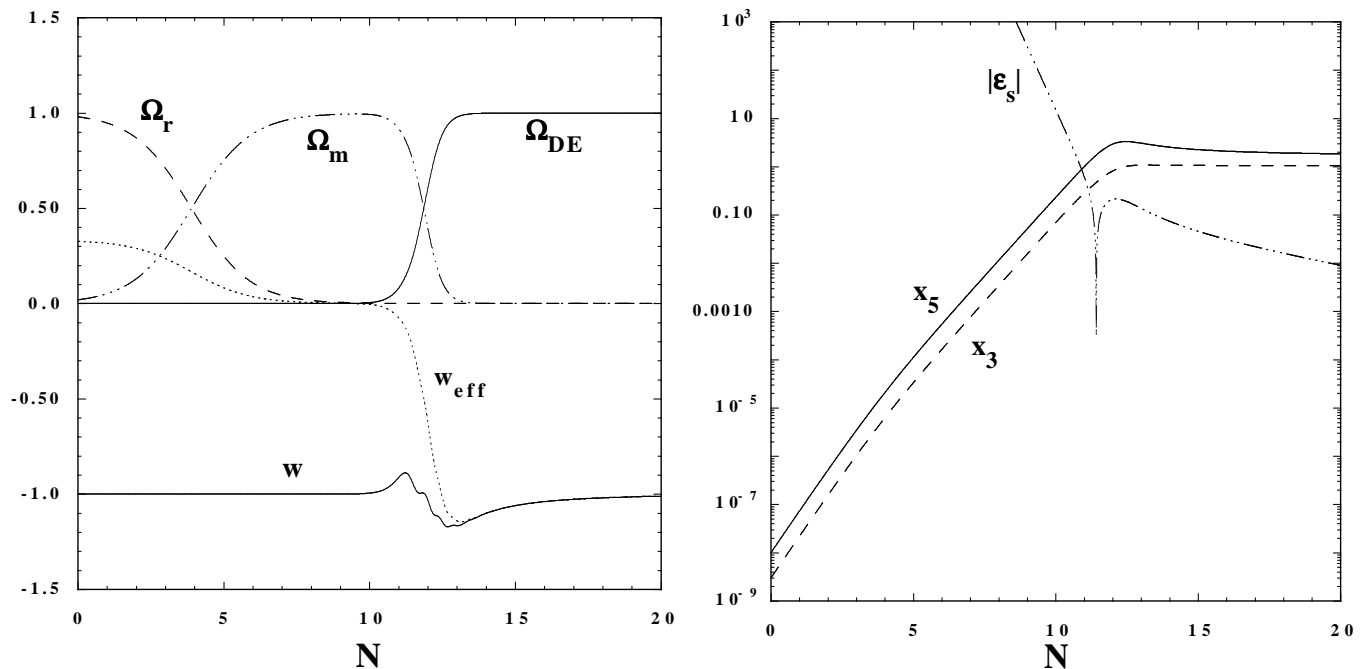


FIG. 1: Cosmological evolution in  $N \equiv \ln a$  for the model parameters  $\alpha = 1$ ,  $\gamma = 1/2$ ,  $\epsilon/m = 3$  and  $M/m = 1$ . We choose initial conditions  $x_1 = 0$ ,  $x_2 = 0$ ,  $x_3 = 3 \times 10^{-9}$ ,  $x_4 = 0$ ,  $x_5 = 10^{-8}$  and  $x_6 = 0.99$ . The left panel shows the evolution of  $\Omega_{DE}$ ,  $\Omega_m$ ,  $\Omega_r$ ,  $w$  and  $w_{\text{eff}}$ , whereas the right panel shows the evolution of  $x_3$  and  $x_5$  together with the slow-roll parameter  $\epsilon_s$ . After the cosmological constant boundary crossing, the DE EOS parameter  $w$  reaches a minimum  $w_{\min} = -1.19$  and then increases towards the de Sitter value  $w = -1$  from the phantom side.

The pattern shown in Fig. 1 is generic in our model, provided that its parameters and initial data obey  $m/\epsilon \ll 1$ ,  $M/\epsilon \ll 1$  and  $x_3/x_5 \ll 1$  (in fact, the inequalities here need not be strong). The strengths of the effects depend, of course, on the values of these parameters. In particular, the minimum value  $w_{\min}$  is related to the slow-roll parameter  $\epsilon_s$  given in Eq. (43). Since  $\rho + p \simeq -M^2 X^2 \xi$  and  $\rho \simeq (1/2)m^2 \phi^2$  during the phantom phase, the EOS parameter  $w$



is approximately given by

$$w + 1 \simeq -\frac{M^2 m_{\text{pl}}^2}{6\pi\epsilon^2\phi^2}\xi. \quad (47)$$

Using Eq. (43) we find that  $w$  is directly related to the slow-roll parameter  $\epsilon_s$ ,

$$w \simeq -1 - \epsilon_s, \quad (48)$$

which is valid only during the phantom period. If the field  $\phi$  evolves very slowly one has  $\epsilon_s \ll 1$ , so  $w_{\text{min}}$  is close to  $-1$ . On the contrary, the appreciable deviation from  $w = -1$  occurs if  $\epsilon_s$  is not very much smaller than unity.

The slow-roll parameter is expressed as follows,

$$\epsilon_s = \frac{2}{9} \left(\frac{m}{\epsilon}\right)^2 \left(\frac{x_5}{x_3}\right)^2 \left(1 - \frac{3\alpha}{x_5^2}\right). \quad (49)$$

Since the field  $\phi$  is practically frozen during the radiation and matter epochs, the ratio  $x_5/x_3 = \sqrt{6}M/(\kappa m\phi)$  is practically constant. The main change of  $\epsilon_s$  during these epochs comes from the variation of the term  $3\alpha/x_5^2$ . The parameter  $\epsilon_s$  is large and negative,  $|\epsilon_s| \gg 1$ , at the initial stage ( $x_5 \ll 1$ ) and then changes the sign if the variable  $x_5 = M/H$  becomes larger than  $\sqrt{3\alpha}$ . Then  $\epsilon_s$  reaches a maximum around the time at which  $H$  has a minimum, after which  $\epsilon_s$  decreases towards zero with the increase of  $H$  to the de Sitter point (A). This behaviour is clearly seen in the right panel of Fig. 1.

Equation (49) implies that for smaller  $m/\epsilon$  one gets smaller absolute value of  $\epsilon_s$  at its minimum, leading to the value of  $w_{\text{min}}$  closer to  $-1$ . This is shown in Fig. 2. From Fig. 1 it is clear, however, that the minimum of  $w$  occurs after the present epoch ( $\Omega_m \simeq 0.3$ ,  $\Omega_{\text{DE}} \simeq 0.7$ ). Again, this is a rather generic feature of our model. Therefore, instead of  $w_{\text{min}}$ , more interesting quantities are the present value  $w_0$  of the DE EOS parameter and also its maximum value before the cosmological constant boundary crossing. These quantities are also shown in Fig. 2. Overall, the behaviour shown in Fig. 1 is more pronounced at larger  $m/\epsilon$ , once other parameters of solutions are kept fixed.

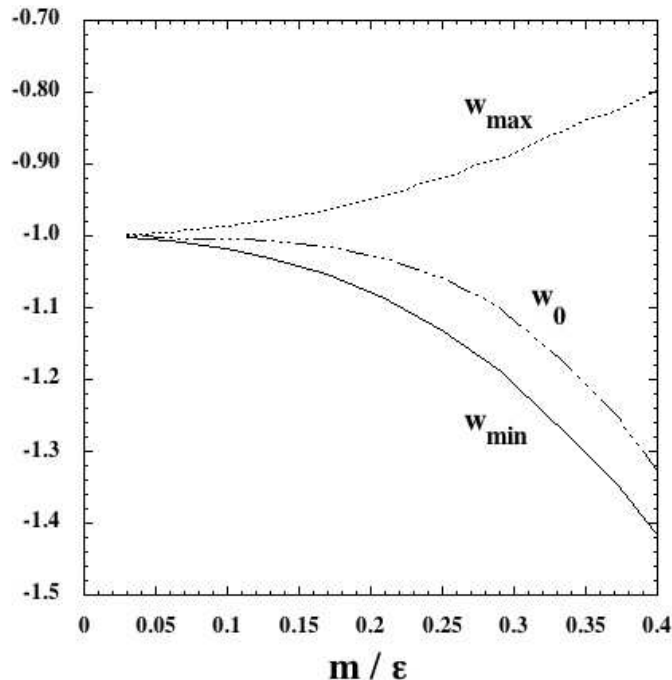


FIG. 2: The minimum value of the EOS parameter  $w$  of DE, its value  $w_0$  at the present epoch ( $\Omega_m = 0.3$ ,  $\Omega_{\text{DE}} = 0.7$ ) and its maximum value as functions of  $m/\epsilon$  for  $M/\epsilon = 1/30$  and the initial value  $x_3/x_5 = 0.3$ ,  $x_1 = x_2 = x_4 = 0$  and  $x_6 = 0.99$ .

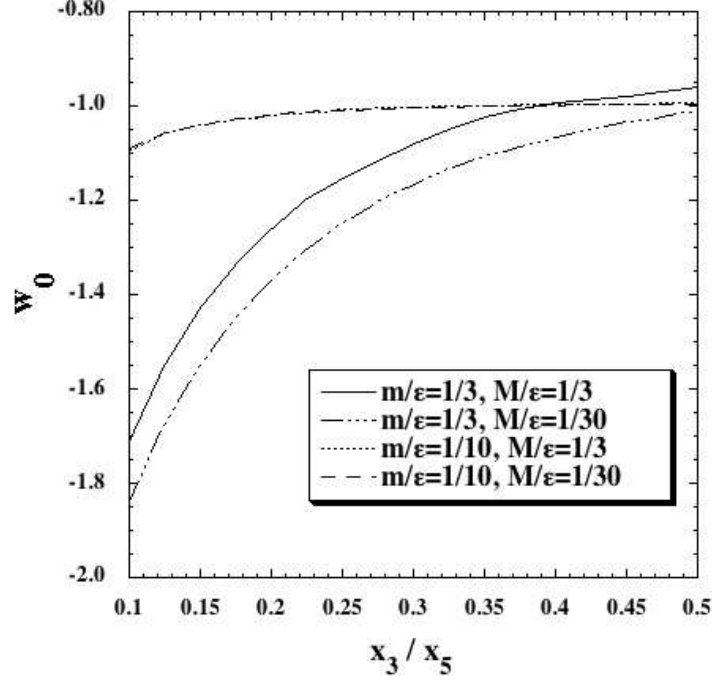


FIG. 3: The dependence of the present value  $w_0$  (i.e.,  $w$  at  $\Omega_m = 0.3$ ,  $\Omega_{DE} = 0.7$ ) on the initial value of  $x_3/x_5 = (\kappa m\phi)/(\sqrt{6}M)$ , for different sets of the model parameters. Other initial conditions are the same as in Fig. 2.

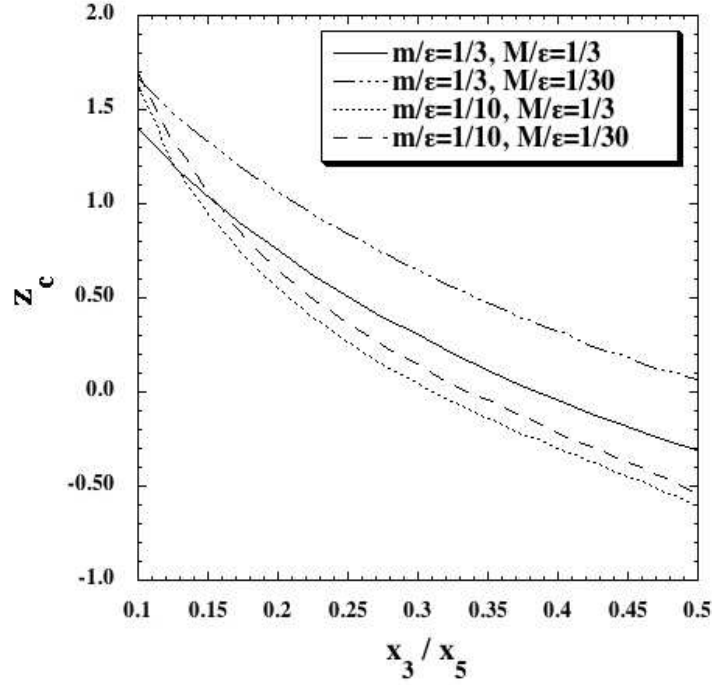


FIG. 4: The dependence of the redshift (from the present epoch,  $\Omega_m = 0.3$ ,  $\Omega_{DE} = 0.7$ ) of the cosmological constant boundary crossing,  $w = -1$ , on the initial value of  $x_3/x_5 = (\kappa m\phi)/(\sqrt{6}M)$ . Other initial conditions are the same as in Fig. 2.

The initial ratio  $x_3/x_5$ , i.e., the initial value of the field  $\phi$  is also important to determine the amplitude of  $\varepsilon_s$ . Since this ratio is practically constant before the dark energy epoch, a smaller initial ratio  $x_3/x_5$  results in a stronger deviation of  $w_{\min}$  from  $-1$ . The present value  $w_0$  also becomes more negative (stronger deviating from  $-1$ ), while the cosmological constant boundary crossing occurs earlier. At relatively large values of  $m/\epsilon$  the increase of  $M$  has the opposite effect, while at smaller  $m/\epsilon$  the effects due to the variation of  $M$  are small. These properties are illustrated in Figs. 3 and 4.

From Eq. (39) the phantom phase is characterized by  $x_5 > \sqrt{3\alpha} = \mathcal{O}(1)$ . If the initial conditions are chosen in such a way as to satisfy  $x_3 \ll x_5$ , at the time when the variable  $x_3$  becomes of order unity,  $x_5$  is larger than unity so that the condition for the existence of the phantom epoch is indeed realized. In fact, the condition  $x_3 \ll x_5$  translates into

$$\phi \ll \sqrt{\frac{3}{4\pi}} \frac{M}{m} m_{\text{pl}}, \quad (50)$$

which is similar to the upper bound given in Eq. (44). The right panel of Fig. 1 corresponds to this type of the cosmological evolution giving  $w_{\min} < -1$ . The variable  $x_5$  reaches a maximum value larger than  $\sqrt{3\alpha}$  and then decreases and finally approaches the de Sitter point (A).

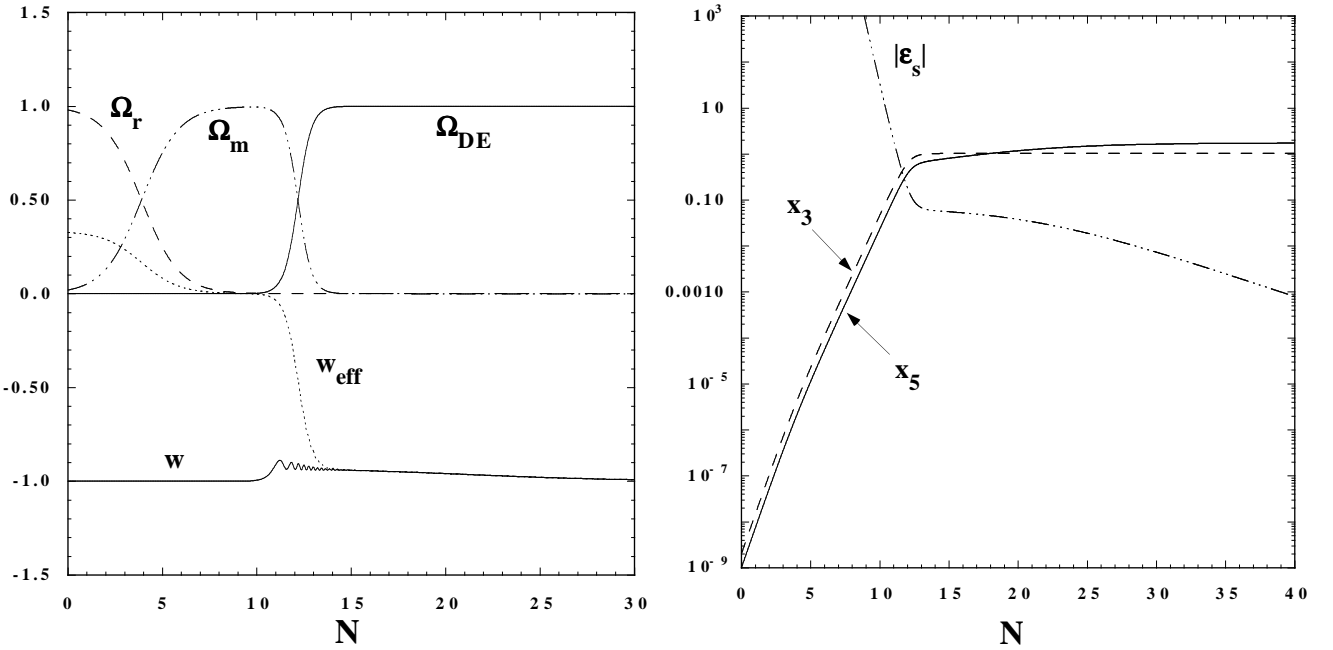


FIG. 5: Cosmological evolution for the model parameters  $\alpha = 1$ ,  $\gamma = 1/2$ ,  $\epsilon/m = 3$  and  $M/m = 0.1$ . We choose initial conditions  $x_1 = 0$ ,  $x_2 = 0$ ,  $x_3 = 2 \times 10^{-9}$ ,  $x_4 = 0$ ,  $x_5 = 10^{-9}$  and  $x_6 = 0.99$ . In this case the cosmological constant boundary crossing is not realized because  $x_3$  becomes of order unity before  $x_5$  gets larger than  $\sqrt{3\alpha}$ .

On the other hand, for the initial conditions  $x_3 \gtrsim x_5$ , at the time when  $x_3$  becomes of order unity,  $x_5$  is still smaller than unity. The variable  $x_5$  continues to grow towards the value  $x_5 = \sqrt{3\alpha}$  without reaching the phantom region. Hence the system does not cross the boundary  $w = -1$ . In Fig. 5 we plot the cosmological evolution for the initial conditions  $x_3 = 2 \times 10^{-9}$  and  $x_5 = 10^{-9}$  for the model parameters  $\epsilon/m = 3$  and  $M/m = 0.1$ . In this case the DE EOS parameter is always in the region  $w > -1$ . From the right panel of Fig. 5 it is seen that the variable  $x_5$  continues to grow towards  $x_5 = \sqrt{3\alpha}$  without crossing this border, and that  $\varepsilon_s$  does not cross zero.

At the end of this section we discuss the variation of the effective gravitational constant. According to Eq. (6), the effective Newton's constant that determines the interaction deep inside the horizon scale is given by

$$G_* = G(1 - 4\pi G\alpha X^2)^{-1}. \quad (51)$$

Its variation in time is conveniently expressed in terms of the following quantity

$$\frac{G_{*,N}}{G_*} \equiv \frac{\dot{G}_*}{G_* H} = \frac{8\pi\alpha X X_{,N}}{m_{\text{pl}}^2(1 - 3\alpha x_4^2)} = \frac{6\alpha x_1 x_4}{\sqrt{\gamma}(1 - 3\alpha x_4^2)}. \quad (52)$$

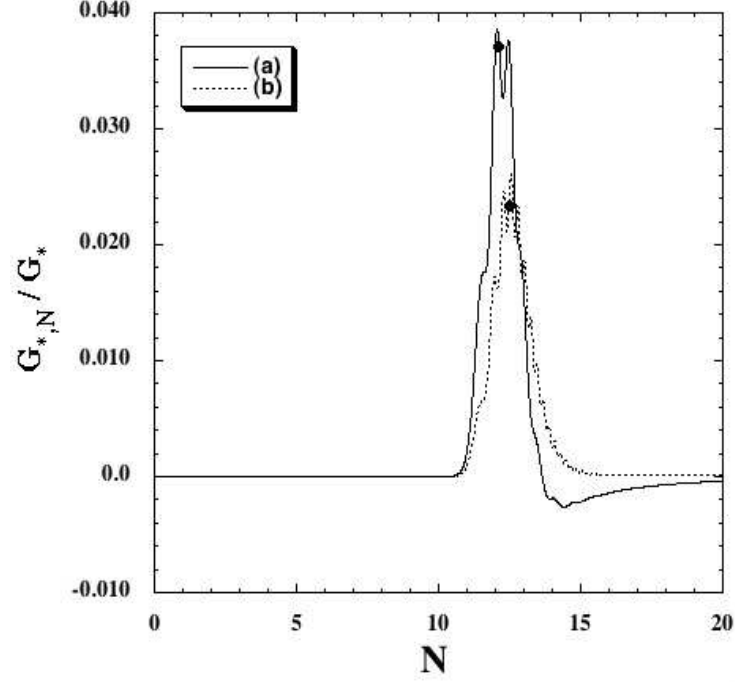


FIG. 6: The evolution of the variation of the effective gravitational constant  $G_{*,N}/G_*$ . The cases (a) and (b) correspond to the model parameters and initial conditions given of Figs. 1 and 5, respectively. The black points represent the values at the present epoch ( $\Omega_m \simeq 0.3$ ).

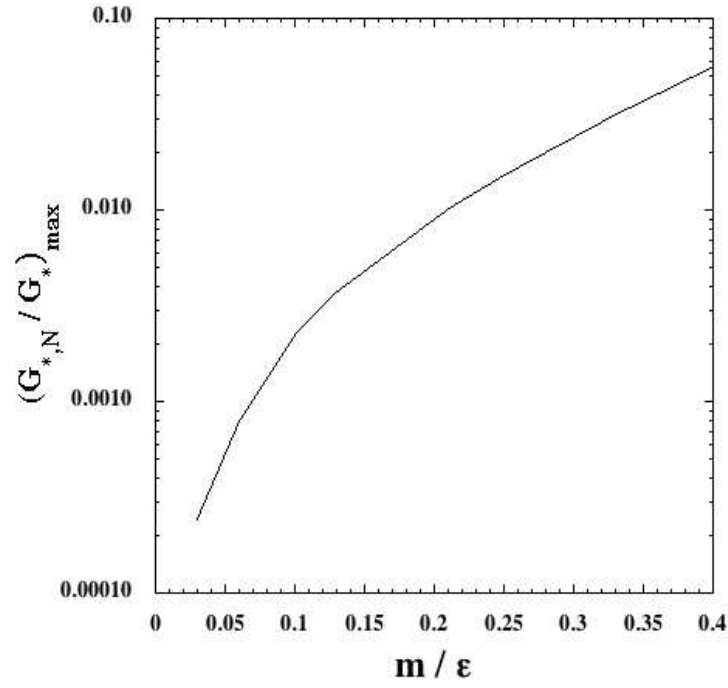


FIG. 7: The maximum value of  $G_{*,N}/G_*$  as a function of  $m/\epsilon$ . Other parameters and initial conditions are the same as in Fig. 2.

The typical experimental and observational constraints on the variation of  $G_*$  in the present Universe are given by  $|\dot{G}_*/G_*| \lesssim 10^{-12} \text{yr}^{-1}$  [37], which translates into the condition

$$\left| \dot{G}_*/G_* \right| \lesssim 10^{-2} H_0. \quad (53)$$

In Fig. 6 we plot the evolution of the quantity  $G_{*,N}/G_*$  for the model parameters and initial conditions given in Figs. 1 and 5. At the present epoch ( $\Omega_m \simeq 0.3$ ) we obtain the values  $\dot{G}_*/G_* = 3.5 \times 10^{-2} H_0^{-1}$  and  $2.4 \times 10^{-2} H_0^{-1}$  for these two cases, respectively. Comparing Fig. 6 with left panels of Fig. 1 and 5 one observes that the variation of the gravitational constant is correlated in time with the deviation of  $w$  from  $-1$ . This is clear from Eq. (51) too: the gravitational constant varies when the fields  $X$  changes in time, while the latter occurs during the transition from the matter dominated stage to the final de Sitter attractor. It is precisely at this transition stage that  $w$  substantially deviates from  $-1$ .

Figure 7 shows the maximum value of  $\dot{G}_*/(G_*H)$  as a function of  $m/\epsilon$ . Again, the variation of the effective Newton's constant is more pronounced at larger  $m/\epsilon$ . This means that it is correlated with the amplitude of the deviation of  $w$  from  $-1$ . The dependence of  $\dot{G}_*/(G_*H)$  on  $M$  and on the initial value of  $x_3/x_5$  is rather weak.

It is worth pointing out that as long as the deviation of the EOS from  $w = -1$  is not so significant, the models satisfy the constraint (53), and also that our model predicts the variation of  $G_*$  which is close to the present upper bound on  $\dot{G}_*/G_*$ .

#### IV. MOMENTUM SCALES OF INSTABILITIES

In this section we study the momentum scales of instabilities present in our model.

##### A. Minkowski spectrum

Let us first study the dispersion relations in Minkowski space-time. We consider the perturbations for the fields,

$$B_0 = X + b_0, \quad B_i = b_i, \quad \Phi = \phi + \varphi. \quad (54)$$

The quadratic Lagrangian for perturbations, following from the general expression (1), is

$$\begin{aligned} \mathcal{L}_{b_0, b_i, \varphi} = & \frac{\gamma}{2} \partial_\mu b_0 \partial^\mu b_0 + \frac{\alpha}{2} \partial_\mu b_i \partial^\mu b_i + \frac{1}{2} \partial_\mu \varphi \partial^\mu \varphi + \epsilon \partial_0 \varphi b_0 - \epsilon \partial_i \varphi b_i \\ & - \frac{1}{2} m_0^2 b_0^2 - \frac{1}{2} m_1^2 b_i^2 - \frac{1}{2} m_\varphi^2 \varphi^2, \end{aligned} \quad (55)$$

where

$$m_0^2 = U_{,XX}, \quad m_1^2 = -\frac{U_{,iX}}{X}, \quad m_\varphi^2 = W_{,\phi\phi}. \quad (56)$$

For our model (15) one has  $-m_0^2 = m_1^2 = M^2$  and  $m_\varphi^2 = m^2$ . In what follows we concentrate on this case, and assume the following relations, see (40) and (45),

$$\begin{aligned} \epsilon & \gg \sqrt{\alpha} m, \\ \epsilon & \gg M. \end{aligned} \quad (57)$$

Varying the Lagrangian (55) with respect to  $b_i$ ,  $b_0$  and  $\varphi$ , we obtain the equations for the field perturbations. In order to find the spectrum of the system we write the solutions in the form  $b_0 = \tilde{b}_0 e^{i\mathbf{p}\mu\mathbf{x}^\mu} = \tilde{b}_0 e^{i(\omega t - \mathbf{P}\cdot\mathbf{r})}$ ,  $b_i = \tilde{b}_i e^{i\mathbf{p}\mu\mathbf{x}^\mu}$  and  $\varphi = \tilde{\varphi} e^{i\mathbf{p}\mu\mathbf{x}^\mu}$ . The transverse mode of the vector field  $B_i$  has the dispersion relation

$$\omega_0^2 = p^2 + \frac{M^2}{\alpha}. \quad (58)$$

The three scalar modes  $\tilde{b}_i = (p_i/p)\tilde{b}_L$ ,  $\tilde{b}_0$  and  $\tilde{\varphi}$  satisfy the following equations

$$\left( \omega^2 - p^2 - \frac{M^2}{\alpha} \right) \tilde{b}_L + i \frac{\epsilon}{\alpha} p \tilde{\varphi} = 0, \quad (59)$$

$$\left( \omega^2 - p^2 + \frac{M^2}{\gamma} \right) \tilde{b}_0 - i \frac{\epsilon}{\gamma} \omega \tilde{\varphi} = 0, \quad (60)$$

$$(\omega^2 - p^2 - m^2) \tilde{\varphi} - i \epsilon \omega \tilde{b}_0 - i \epsilon p \tilde{b}_L = 0. \quad (61)$$

Expressing  $\tilde{b}_L$  and  $\tilde{b}_0$  in terms of  $\tilde{\varphi}$  from Eqs. (59), (60) and plugging them into Eq. (61), we find that the eigenfrequencies corresponding to three mixed states satisfy

$$(z - m^2) \left( z + \frac{M^2}{\gamma} \right) \left( z - \frac{M^2}{\alpha} \right) - \epsilon^2 z \left( \frac{z}{\gamma} + \frac{p^2}{\gamma} + \frac{p^2}{\alpha} - \frac{M^2}{\gamma\alpha} \right) = 0, \quad (62)$$

where

$$z \equiv \omega^2 - p^2. \quad (63)$$

The spectrum in the case  $m = 0$  was studied in Ref. [33]. Our purpose here is to extend the analysis to the case of non-zero  $m$ . Denoting the solutions of Eq. (62) as  $z_1, z_2$  and  $z_3$ , we obtain the relation

$$z_1 z_2 z_3 = -\frac{m^2 M^4}{\alpha\gamma}. \quad (64)$$

Once the conditions (57) are satisfied, then one can show that if the relation

$$z_1 < z_2 < z_3 \quad (65)$$

holds at some momentum, then the inequality (65) is satisfied for all momenta.

In the limits  $p \rightarrow \infty$  and  $p \rightarrow 0$ , we obtain the following dispersion relations, respectively.

- (A) UV limit ( $p \rightarrow \infty$ )

$$\begin{aligned} \omega_1 &= p - \frac{\epsilon}{2} \sqrt{\frac{1}{\gamma} + \frac{1}{\alpha}} + \frac{\epsilon^2}{8p} \left( \frac{2m^2}{\epsilon^2} + \frac{1}{\gamma} - \frac{1}{\alpha} \right) + \mathcal{O}(M^2/p), \\ \omega_2 &= p + \frac{m^2 M^4}{2p^3 \epsilon^2 (\alpha + \gamma)} + \mathcal{O}(1/p^5), \\ \omega_3 &= p + \frac{\epsilon}{2} \sqrt{\frac{1}{\gamma} + \frac{1}{\alpha}} + \frac{\epsilon^2}{8p} \left( \frac{2m^2}{\epsilon^2} + \frac{1}{\gamma} - \frac{1}{\alpha} \right) + \mathcal{O}(M^2/p). \end{aligned} \quad (66)$$

We see that  $\omega_1 < \omega_2 < \omega_3$  and  $z_1 < 0, z_{2,3} > 0$ . In all three cases the group velocities  $\partial\omega_i/\partial p$  are less than 1, so neither mode is superluminal at high three-momenta, provided that  $\alpha > \gamma$ . The two-derivative terms in the Lagrangian (55) dominate in the UV limit, so there are neither ghosts nor tachyons in this limit.

- (B) IR limit ( $p \rightarrow 0$ )

$$\begin{aligned} \omega_1 &= -\frac{m^2 M^2}{\epsilon^2} [1 + \mathcal{O}(m^2/\epsilon^2, M^2/\epsilon^2)], \\ \omega_2 &= \frac{M^2}{\alpha}, \\ \omega_3 &= \frac{\epsilon^2}{\gamma} + m^2 + \mathcal{O}(M^2). \end{aligned} \quad (67)$$

We see again that  $\omega_1 < \omega_2 < \omega_3$  and  $z_1 < 0, z_{2,3} > 0$ . This means that using the property (65) we can identify the modes: the first one has the behaviour (66) and (67), and so on.

It follows from Eq. (64) that  $z_i$  never vanish. In fact the coefficients in Eq. (62) are regular at all momenta, so  $z_i$  are regular as well. Therefore,  $z_i$  never change signs and hence  $z_1 < 0, z_{2,3} > 0$  for all momenta. This means, in particular, that the second and third modes never become tachyonic.

Let us discuss the dangerous mode with the dispersion relation  $\omega = \omega_1(p)$  in some detail. The expression for the fields in each mode is

$$\begin{aligned} \tilde{b}_{L,i} &= -i\epsilon p (\gamma z_i + M^2) \cdot C_i, \\ \tilde{b}_{0,i} &= i\epsilon \omega (\alpha z_i - M^2) \cdot C_i, \\ \tilde{\varphi}_i &= (\gamma z_i + M^2)(\alpha z_i - M^2) \cdot C_i, \end{aligned} \quad (68)$$

where  $C_i$  are the normalization factors. Setting  $\omega^2 = 0$  in Eq. (62), we obtain three critical momenta

$$p_{1,2}^2 = \frac{1}{2} \left[ \frac{\epsilon^2 - M^2}{\alpha} - m^2 \pm \sqrt{\left( \frac{\epsilon^2 - M^2}{\alpha} - m^2 \right)^2 - \frac{4m^2 M^2}{\alpha}} \right], \quad (69)$$

$$p_3^2 = \frac{M^2}{\gamma}. \quad (70)$$

Under the conditions (57), the critical momenta  $p_{1,2}^2$  are approximately given by

$$p_1^2 \simeq \frac{\epsilon^2 - M^2}{\alpha} - m^2, \quad p_2^2 \simeq \frac{m^2 M^2}{\epsilon^2}, \quad (71)$$

so that  $p_1^2 > p_3^2 > p_2^2 > 0$ . The tachyonic mode ( $\omega_1^2 < 0$ ) is present for  $0 < p^2 < p_2^2$  and  $p_3^2 < p^2 < p_1^2$ .

In order to find whether there are ghosts we calculate the energy of the modes (68),

$$E_i(p) = 2\omega^2 |C_i|^2 \left[ \alpha \epsilon^2 p^2 (\gamma z_i + M^2)^2 + \epsilon^2 (\gamma p^2 - M^2) (\alpha z_i - M^2)^2 + (\gamma z_i + M^2)^2 (\alpha z_i - M^2)^2 \right].$$

For the modes with  $\omega_{2,3}$  we have  $E_{2,3}(p) > 0$ . For the mode with  $\omega_1$  the energy is equal to zero at  $p = p_3 = M/\sqrt{\gamma}$ . While  $\omega_1^2 > 0$  for  $p^2 < p_3^2 \equiv M^2/\gamma$ , the energy  $E_1(p)$  changes its sign at this momentum. Thus the mode with  $\omega_1$  is a ghost for  $p^2 < M^2/\gamma$ .

We summarize the properties of the dangerous mode as follows:

- (i)  $p^2 > (\epsilon^2 - M^2)/\alpha - m^2$ : healthy
- (ii)  $M^2/\gamma < p^2 < (\epsilon^2 - M^2)/\alpha - m^2$ : tachyon
- (iii)  $m^2 M^2/\epsilon^2 < p^2 < M^2/\gamma$ : ghost, but not tachyon
- (iv)  $0 < p^2 < m^2 M^2/\epsilon^2$ : tachyon.

Unlike the case  $m = 0$  [33] the tachyon is present in the deep IR region (iv).

To end up the discussion of the modes in Minkowski space-time, we give the expressions for the minimum values of  $\omega^2$  in the tachyonic regions,

- (ii):

$$\omega_{\min}^2 = -\frac{\gamma \epsilon^2}{4\alpha(\alpha + \gamma)} \quad \text{at} \quad p^2 = \frac{\epsilon^2}{4\alpha} \frac{\gamma + 2\alpha}{\gamma + \alpha}. \quad (72)$$

- (iv):

$$\omega_{\min}^2 = -\frac{m^2 M^2}{\epsilon^2} \quad \text{at} \quad p^2 = 0.$$

Note that  $|\omega_{\min}^2|$  is relatively large in the region (ii), so this region is the most problematic.

## B. Evolution of perturbations in cosmological background

Finally we discuss the evolution of field perturbations in the FRW background (2). In the cosmological context the physical momentum  $p$  is related to the comoving momentum  $k$  as  $p = k/a$ . Once the parameters of the model and initial data are such that the cosmological boundary crossing occurs, the present epoch ( $\Omega_{\text{DE}} \simeq 0.7$ ) typically corresponds to the phantom region. From Fig. 1 we see that the variable  $x_5 = M/H$  does not change much during the transition from the phantom epoch to the final de Sitter era. Hence the present value of the Hubble parameter ( $H_0$ ) is of the same order as the value  $H = M/\sqrt{3\alpha}$  at the de Sitter point (A). This means that the value  $p_3 = M/\sqrt{\gamma}$  is of the same order as  $H_0$  provided that  $\gamma$  and  $\alpha$  are of order unity.

The tachyon appears when the momentum  $p = k/a$  of the dangerous mode becomes smaller than  $\sqrt{(\epsilon^2 - M^2)/\alpha - m^2}$  and temporally disappears when the mode crosses the value  $M/\sqrt{\gamma}$ . Hence this instability is present for the modes which are inside the Hubble radius and satisfy  $M/\sqrt{\gamma} < p < \sqrt{(\epsilon^2 - M^2)/\alpha - m^2}$ , but it

is absent for the modes deep inside the Hubble radius, satisfying  $p > \sqrt{(\epsilon^2 - M^2)/\alpha - m^2}$ . After the Hubble radius crossing ( $k = aH$ ), the tachyonic instability disappears in the momentum region  $m^2 M^2/\epsilon^2 < p^2 < M^2/\gamma$ , but the tachyon appears again for  $p^2 < m^2 M^2/\epsilon^2$ . Note that the ghost existing at  $m^2 M^2/\epsilon^2 < p^2 < M^2/\gamma$  is not a problem because of its low energy [13, 40].

In what follows we discuss the evolution of field perturbations in the two tachyonic regimes. Before doing that it is instructive to study the high-momentum regime that sets the initial data for the tachyonic evolution.

$$1. \quad p^2 \gg (\epsilon^2 - M^2)/\alpha - m^2$$

We denote the overall amplitude of the dangerous mode as  $\varphi$ . Since the modes are deep inside the Hubble radius ( $k/a \gg H$ ) in the regime we discuss here, the field perturbation  $\chi$  approximately satisfies

$$\frac{d^2}{d\eta^2}\chi + k^2\chi \simeq 0, \quad (73)$$

where  $\chi = a\varphi$  and  $\eta$  is conformal time defined by  $\eta = \int a^{-1}dt$ . Taking the asymptotic Minkowski vacuum state,  $\chi = e^{-ik\eta}/\sqrt{2k}$ , the squared amplitude of the field perturbation  $\varphi$  is given by [41]

$$\mathcal{P}_\varphi = \frac{4\pi k^3}{(2\pi)^3} |\varphi|^2 = \left(\frac{k}{2\pi a}\right)^2. \quad (74)$$

Since the maximum momentum at which the tachyon appears is  $k/a \simeq \epsilon/\sqrt{\alpha}$ , one has the following estimate for the amplitude of the field perturbation at the beginning of the tachyonic instability,

$$\varphi_i \simeq \frac{\epsilon}{2\pi\sqrt{\alpha}}. \quad (75)$$

As usual, this amplitude characterizes the contribution of a logarithmic interval of momenta into  $\langle \varphi^2(\mathbf{x}) \rangle$ .

$$2. \quad M^2/\gamma < p^2 < (\epsilon^2 - M^2)/\alpha - m^2$$

This interval of momenta is dangerous, as the perturbations undergo the tachyonic amplification. Since the modes are still inside the Hubble radius, one can neglect the gravitational effects on the ‘‘frequency’’  $\omega$  when estimating the growth of field perturbations. By the time the tachyonic amplification ends up, the amplitude of field perturbations is estimated as

$$\varphi \simeq \varphi_i \exp\left(\int_{t_i}^{t_f} |\omega_1| dt\right) = \varphi_i \exp\left(\int_{p_1}^{p_3} \frac{|\omega_1|}{H} \frac{dp}{p}\right). \quad (76)$$

Recall that  $p_1 \simeq \epsilon/\sqrt{\alpha}$  and  $p_3 = M/\sqrt{\gamma}$ . The largest value of  $|\omega_1^2|$  is approximately given by (72). Substituting this value into Eq. (76) and recalling that the background changes slowly ( $H \simeq \text{const}$ ), one finds that the amplitude of the field perturbation after exit from the tachyonic regime is of order

$$\varphi \simeq \frac{\epsilon}{2\pi\sqrt{\alpha}} \exp\left[\frac{1}{2}\sqrt{\frac{\gamma}{\alpha(\gamma+\alpha)}} \frac{\epsilon}{H} \log\left(\sqrt{\frac{\gamma}{\alpha}} \frac{\epsilon}{M}\right)\right], \quad (77)$$

where we used Eq. (75).

Recall now that  $H$  is of the same order as  $M/\sqrt{3\alpha}$  during the phantom phase. Hence the large ratio  $\epsilon/M$  leads to a strong amplification of field perturbations. Since the parameter  $x_3 = \kappa m\phi/\sqrt{6}H$  is of order unity at the phantom and de Sitter phase, the homogeneous field  $\phi$  is estimated as  $\phi \simeq \sqrt{\frac{3}{4\pi}} \frac{H m_{\text{pl}}}{m}$ . The requirement that the perturbation  $\varphi$  is smaller than the background field  $\phi$  leads to the constraint

$$\exp\left[\frac{1}{2}\sqrt{\frac{\gamma}{\alpha(\gamma+\alpha)}} \frac{\epsilon}{H} \log\left(\sqrt{\frac{\gamma}{\alpha}} \frac{\epsilon}{M}\right)\right] < \sqrt{3\alpha\pi} \frac{H m_{\text{pl}}}{\epsilon m}. \quad (78)$$

As an example, in the case  $m = H_0 = 10^{-42}$  GeV,  $M = \sqrt{3\alpha}H_0$ ,  $\alpha = 1$  and  $\gamma = 1/2$ , we obtain the constraint  $\epsilon/M \lesssim 70$ . As long as  $\alpha$  and  $\gamma$  are of order one, the ratio  $\epsilon/M$  should not be too much larger than unity.



$$3. \quad 0 < p^2 < m^2 M^2 / \epsilon^2$$

After the Hubble radius crossing, the effect of the cosmic expansion can no longer be neglected when estimating the “frequencies” of the field perturbations. Since there are no tachyonic instabilities for  $m^2 M^2 / \epsilon^2 < p^2 < M^2 / \gamma$ , we consider the evolution of perturbations in the region  $0 < p^2 < m^2 M^2 / \epsilon^2$ . In Ref. [33] the equations for the field perturbations were derived in the slow-rolling background under the condition  $p^2 \ll M^2, m^2$  by neglecting the back reaction of metric perturbations. The equation for the perturbation  $\chi = a\varphi$  is approximately given by

$$\frac{d^2}{d\eta^2}\chi + \left( k^2 - \frac{1}{a} \frac{d^2 a}{d\eta^2} - a^2 \frac{m^2 M^2}{\epsilon^2} \right) \chi = 0. \quad (79)$$

The last term corresponds to the tachyonic mass term, which already appeared in Minkowski spacetime [see Eq. (67)]. Since the term  $(d^2 a / d\eta^2) / a$  is of order  $a^2 H^2$ , one can estimate the ratio of the tachyonic mass relative to this gravitational term:

$$\delta \equiv \frac{a^2 m^2 M^2 / \epsilon^2}{(d^2 a / d\eta^2) / a} \simeq \frac{m^2 M^2}{\epsilon^2 H^2}. \quad (80)$$

If we use the de Sitter value  $H = M / \sqrt{3\alpha}$ , this ratio is estimated as  $\delta = 3\alpha m^2 / \epsilon^2 \ll 1$ . Hence the gravitational term  $(d^2 a / d\eta^2) / a$  dominates over the tachyonic mass.

In the de Sitter background with  $a = -1 / (H\eta)$  the approximate solutions to Eq. (79) can be obtained by setting  $\chi = -(C/H)\eta^{-1+\tilde{\delta}}$ . One finds that  $\tilde{\delta} = -m^2 M^2 / (3H^2 \epsilon^2)$  for the growing solution, thereby giving

$$\varphi = C\eta^{-\frac{m^2 M^2}{3H^2 \epsilon^2}} \propto a^{\delta/3}. \quad (81)$$

In Ref. [33] it was shown that the physical temporal component of the vector field perturbations evolves as  $b_0/a \propto a^{\delta/3}$ , whereas the physical spatial component of the vector field decreases as  $B_i/a \propto a^{-1+\delta/3}$ . The growth rate of  $\varphi$  and  $b_0/a$  is small due to the condition  $\delta \ll 1$ . So, the second tachyonic instability is harmless for the past and present cosmological evolution. However, we notice that since the de Sitter point (A) is a late-time attractor, the perturbations  $\varphi$  and  $b_0/a$  become larger than the homogeneous background fields in the distant future.

## V. CONCLUSIONS

In this paper we have studied the dynamics of dark energy in a Lorentz-violating model with the action given in (1). The model involves a vector field  $B_\mu$  and a scalar field  $\Phi$  with mass terms  $M$  and  $m$ , respectively. The presence of the one-derivative term  $\epsilon \partial_\mu \Phi B^\mu$  leads to an interesting dynamics at the IR scales larger than  $\epsilon^{-1}$ . The phantom equation of state can be realized without having ghosts, tachyons or superluminal modes in the UV region.

We have taken into account the contributions of radiation and non-relativistic matter and derived the fixed points of the system. Interestingly, there exists a de Sitter attractor point that can be used for the late-time acceleration. The phantom regime does not correspond to any of the fixed points of the system, but we have found that in a range of parameters, the phantom stage occurs during the transition from the matter epoch to the final de Sitter attractor. As is seen, e.g., in Fig. 1 the equation of state parameter  $w$  of dark energy crosses the cosmological constant boundary towards the phantom region. We clarified the conditions under which the  $w = -1$  crossing is realized together with the existence of the stable de Sitter solution.

In the model studied in this paper, the effective Newton’s constant is time-dependent. We have found, however, that this dependence is typically mild, though for interesting values of parameters it is close to the experimental bounds.

We have also considered the field perturbations in Minkowski spacetime and obtained the momentum scales of instabilities present in the IR region ( $p \lesssim \epsilon$ ). We have found that either tachyons or ghosts appear for the spatial momenta  $p$  smaller than  $\sqrt{(\epsilon^2 - M^2)/\alpha - m^2}$ , while in the UV region there are no unhealthy modes. In the cosmological context the presence of tachyons at the IR scales leads to the amplification of large-scale field perturbations whose wavelengths are roughly comparable to the present Hubble radius. There are two tachyonic regions of spatial momenta in this model: (a) one is sub-horizon and its momenta are characterized by  $M^2/\gamma < p^2 < (\epsilon^2 - M^2)/\alpha - m^2$ ; (b) another is super-horizon and has  $0 < p^2 < m^2 M^2 / \epsilon^2$ . In the region (a) we derived the condition under which the perturbations always remain smaller than the homogenous fields, see Eq. (78). While the existence of the phantom phase requires that  $\epsilon > M$ , the condition (78) shows that  $\epsilon$  cannot be very much larger than  $M$ . Thus the allowed range of  $\epsilon$  is constrained to be relatively narrow. In the tachyonic region (b) the growth of the perturbations is

estimated as  $\varphi \propto a^{\alpha m^2/\epsilon^2}$ . Since the growth rate is suppressed by the factor  $m^2/\epsilon^2$ , this effect is negligible in the past and at present, though the inhomogeneities can start to dominate over the homogenous fields in the distant future.

There are several issues yet to be understood. The presence of the tachyonic instability on sub-horizon scales may lead to the variation of the gravitational potential, which can be an additional source of the late-time integrated Sachs-Wolfe effect on the CMB power spectrum. Another property of this model is the peculiar time-dependence of the effective Newton's constant, which may result in interesting phenomenology.

The model studied in this paper is likely to belong to a wider class of Lorentz-violating theories exhibiting the phantom behaviour (see Refs. [42] for a number of Lorentz-violating models). It would be interesting to understand how generic are the features we found in our particular model — late-time de Sitter attractor, transient phantom stage, time-dependent Newton's constant, sub-horizon tachyons, super-horizon ghosts, etc. One more direction is to modify our model in such a way that it would be capable of describing inflationary epoch rather than the late-time acceleration. Since it is known that the spectra of scalar and tensor perturbations produced during the phantom inflationary phase are typically blue-tilted [43], this model may give rise to some distinct features in the CMB spectrum.

## ACKNOWLEDGEMENTS

This work is supported by RFBR grant (M. L. and V. R., 05-02-17363-a), grant of the President of Russian Federation (M. L. and V. R., NS-7293.2006.2), INTAS grant (M. L., YSF 04-83-3015), grant of Dynasty Foundation awarded by the Scientific Board of ICFPM (M. L.), the European Union through the Marie Curie Research and Training Network UniverseNet (E. P., MRTN-CT-2006-035863) and JSPS (S. T., No. 30318802).

## Appendix A

We are going to find the effective Newton's constant that determines the strength of gravitational interactions at distances shorter than all scales present in our model, including  $\epsilon^{-1}$ ,  $M^{-1}$ ,  $m^{-1}$  as well as the Hubble distance. To this end, we neglect the last two terms in the action (1), and also neglect the time dependence of the background fields  $\phi$  and  $X$ . We also neglect the space-time curvature of the Universe, and therefore consider our model in Minkowski space-time.

Let us impose the gauge  $h_{0i} = 0$ , where  $h_{\mu\nu}$  is the metric perturbation about the Minkowski background. Then the quadratic Lagrangian for perturbations of metric, vector and scalar fields is readily calculated,

$$\begin{aligned}
L = & \frac{1}{2}\alpha \left[ \left( \dot{b}_i + \frac{1}{2}X\partial_i h_{00} \right)^2 - \left( \partial_i b_j - \frac{1}{2}X\dot{h}_{ij} \right)^2 \right] \\
& + \frac{1}{2}\gamma \left[ \left( \dot{b}_0 + \frac{1}{2}X\dot{h}_{00} \right)^2 - \left( \partial_i b_0 + \frac{1}{2}X\dot{h}_{00} \right)^2 \right] \\
& + \frac{1}{2} [\dot{\varphi}^2 - (\partial_i \varphi)^2] .
\end{aligned} \tag{82}$$

where  $X^2 = B_0^2$  is the background value. Clearly the scalar field  $\varphi$  decouples in our approximation, so we will not consider it in what follows.

By varying the quadratic action with respect to  $h_{00}$  and  $h_{ij}$ , one obtains (00)- and (ij)-components of the linearized energy-momentum tensor for perturbations (note that  $T^{\mu\nu} = -2\delta S/\delta h_{\mu\nu}$ ). Specifying further to scalar perturbations with  $b_i = \partial_i b_L$  and choosing conformal Newtonian gauge,  $h_{00} = 2\Phi$ ,  $h_{ij} = -2\Psi\delta_{ij}$ , one obtains (we keep the standard notation for the Newtonian potential, even though the same notation was used for the original scalar field in the main text)

$$\begin{aligned}
T_0^0 &= \alpha X(X\Delta\Phi - \Delta\dot{b}_L) + \gamma X\Box(b_0 + X\Phi) , \\
T_j^i &= \alpha X\partial_i\partial_j\dot{b}_L - \delta_{ij}\alpha X^2\ddot{\Psi} ,
\end{aligned} \tag{83}$$

where  $\Delta = \partial_i\partial_i$  and  $\Box = \partial_0^2 - \Delta$ . The field equations for  $b_0$  and  $b_L$  in the absence of sources for these fields read

$$\begin{aligned}
\Box(b_0 + X\Phi) &= 0 , \\
-\Box b_L + X(\dot{\Phi} - \dot{\Psi}) &= 0 .
\end{aligned} \tag{84}$$

Now, the longitudinal (proportional to  $\partial_i\partial_j$ ) part of the  $(ij)$ -component of the Einstein equations, in the absence of external anisotropic stresses, gives

$$\Phi + \Psi = 8\pi G\alpha X \dot{b}_L, \quad (85)$$

while the trace part and (00)-component are

$$\ddot{\Psi} + \frac{1}{2}\Delta(\Phi + \Psi) = -4\pi G\alpha X^2 \ddot{\Psi} - 4\pi G p_{ext}, \quad (86)$$

$$-\Delta\Psi = 4\pi G(\alpha X^2 \Delta\Phi - \alpha X \Delta\dot{b}_L) + 4\pi G \rho_{ext}, \quad (87)$$

where  $\rho_{ext}$  and  $p_{ext}$  are energy density and pressure of an external source.

For time-independent, pressureless source it is consistent to take all perturbations independent of time and set  $b_L = 0$ . Then one finds, as usual,  $\Psi = -\Phi$  and obtains the following equation for the Newtonian potential,

$$(1 - 4\pi G\alpha X^2)\Delta\Phi = 4\pi G \rho_{ext}. \quad (88)$$

Thus, the effective Newton's constant in the background field  $X$  is

$$G_* = G(1 - 4\pi G\alpha X^2)^{-1}. \quad (89)$$

This means that the effective Planck mass entering the Newton's law is given by (6).

## Appendix B

In this Appendix we study the stability of the fixed points by considering linear perturbations  $\delta x_i$ . By perturbing Eqs. (23)-(27) we obtain

$$\begin{aligned} \delta x'_1 = & \left(-3 - \frac{H'}{H} - c_1 x_1\right) \delta x_1 + \left(\frac{\epsilon}{M} \frac{1}{\sqrt{\gamma}} x_5 - c_2 x_1\right) \delta x_2 - c_3 x_1 \delta x_3 \\ & + \left(\frac{1}{\sqrt{\gamma}} x_5^2 - \frac{3\alpha}{\sqrt{\gamma}} - c_4 x_1\right) \delta x_4 + \left(\frac{\epsilon}{M} \frac{1}{\sqrt{\gamma}} x_2 + \frac{2}{\sqrt{\gamma}} x_4 x_5 - c_5 x_1\right) \delta x_5 - c_6 x_1 \delta x_6, \end{aligned} \quad (90)$$

$$\begin{aligned} \delta x'_2 = & -\left(\frac{\epsilon}{M} \frac{1}{\sqrt{\gamma}} x_5 + c_1 x_2\right) \delta x_1 - \left(3 + c_2 x_2 + \frac{H'}{H}\right) \delta x_2 - \left(\frac{m}{M} x_5 + c_3 x_2\right) \delta x_3 \\ & - \left(3 \frac{\epsilon}{M} x_5 + c_4 x_2\right) \delta x_4 - \left(\frac{\epsilon}{M} \frac{1}{\sqrt{\gamma}} x_1 + 3 \frac{\epsilon}{M} x_4 + \frac{m}{M} x_3 + c_5 x_2\right) \delta x_5 - c_6 x_2 \delta x_6, \end{aligned} \quad (91)$$

$$\delta x'_3 = -c_1 x_3 \delta x_1 + \left(\frac{m}{M} x_5 - c_2 x_3\right) \delta x_2 - c_3 x_3 \delta x_3 - c_4 x_3 \delta x_4 + \left(\frac{m}{M} x_2 - c_5 x_3\right) \delta x_5 - c_6 x_3 \delta x_6, \quad (92)$$

$$\delta x'_4 = \frac{1}{\sqrt{\gamma}} \delta x_1, \quad (93)$$

$$\delta x'_5 = -c_1 x_5 \delta x_1 - c_2 x_5 \delta x_2 - c_3 x_5 \delta x_3 - c_4 x_5 \delta x_4 - \left(\frac{H'}{H} + c_5 x_5\right) \delta x_5 - c_6 x_5 \delta x_6, \quad (94)$$

$$\delta x'_6 = -c_1 x_6 \delta x_1 - c_2 x_6 \delta x_2 - c_3 x_6 \delta x_3 - c_4 x_6 \delta x_4 - c_5 x_6 \delta x_5 - \left(2 + \frac{H'}{H} + c_6 x_6\right) \delta x_6, \quad (95)$$

where  $\delta(H'/H) = \sum_{i=1}^6 c_i \delta x_i$  with

$$\begin{aligned} c_1 = & -\frac{3x_1 + 6(\alpha/\sqrt{\gamma})x_4}{1 + 3\alpha x_4^2} x_4, \quad c_2 = -\frac{3x_2 + 3(\epsilon/M)x_4 x_5}{1 + 3\alpha x_4^2}, \quad c_3 = \frac{3x_3}{1 + 3\alpha x_4^2}, \\ c_4 = & -\frac{3x_4(3\alpha + x_5^2) + 3(\epsilon/M)x_2 x_5 + 6(\alpha/\sqrt{\gamma})x_1}{1 + 3\alpha x_4^2} - \frac{6\alpha x_4}{1 + 3\alpha x_4^2} \frac{H'}{H}, \\ c_5 = & -\frac{3x_4^2 x_5 + 3(\epsilon/M)x_2 x_4}{1 + 3\alpha x_4^2}, \quad c_6 = -\frac{x_6}{1 + 3\alpha x_4^2}. \end{aligned} \quad (96)$$

The stability of fixed points can be analyzed by considering eigenvalues of the  $6 \times 6$  matrix  $\mathcal{M}$  for perturbations along the lines of Ref. [6, 38].

The stability of the de Sitter point (A) is already presented in the text. Indeed, the spatially homogeneous perturbations are subclass of the perturbations studied in Sec. IV.

For another de Sitter point (B), the eigenvalues are

$$-3, -3, -\frac{3}{2} \pm \frac{1}{2} \sqrt{9 - \frac{12\alpha}{\gamma}}, 0, -1/2, \quad (97)$$

This means that this point is marginally stable. The zero eigenvalue comes from the perturbation equation for  $\delta x_5$ . If  $H$  continues to increase toward the solution (B), this eigenvalue actually obtains a small negative value, as can be seen from Eq. (94). Thus in such a case the point (B) is stable. However, we know that the phantom phase is realized only for finite field values bounded by (44). Hence it is not possible that the actual solutions approach the point (B) with infinite  $H$  and  $\phi$ .

The matter point (C) has the eigenvalues

$$3/2, -3/2, -\frac{4}{3} \pm \sqrt{9 - \frac{48\alpha}{\gamma}}, 0, -1/2, \quad (98)$$

which shows that the matter era correspond to a saddle point with one positive eigenvalue. Hence the solutions eventually repel away from this fixed point even if they temporarily approach it.

The radiation point (D) has the eigenvalues

$$-\frac{1}{2} \pm \frac{1}{2} \sqrt{1 - \frac{12\alpha}{\gamma}}, -1, 0, 2, 1. \quad (99)$$

One finds that the radiation epoch corresponds to a saddle point with two positive eigenvalues.

The kinetic points (E1) and (E2) have the eigenvalues

$$3, 3, 1, 0, \sqrt{\frac{3\alpha}{\gamma}}i, -\sqrt{\frac{3\alpha}{\gamma}}i, \quad (100)$$

which shows that they are unstable.

The above stability analysis shows that the sequence of radiation, matter and de Sitter epochs can indeed be realized.

- 
- [1] A. G. Riess *et al.*, *Astron. J.* **116**, 1009 (1998); *Astron. J.* **117**, 707 (1999); S. Perlmutter *et al.*, *Astrophys. J.* **517**, 565 (1999); P. Astier *et al.*, *Astron. Astrophys.* **447**, 31 (2006); W. M. Wood-Vasey *et al.*, arXiv:astro-ph/0701041.
- [2] D. N. Spergel *et al.* [WMAP Collaboration], *Astrophys. J. Suppl.* **148**, 175 (2003); D. N. Spergel *et al.*, arXiv:astro-ph/0603449.
- [3] U. Seljak *et al.* [SDSS Collaboration], *Phys. Rev. D* **71**, 103515 (2005); M. Tegmark *et al.*, *Phys. Rev. D* **74**, 123507 (2006).
- [4] D. J. Eisenstein *et al.* [SDSS Collaboration], *Astrophys. J.* **633**, 560 (2005).
- [5] V. Sahni and A. A. Starobinsky, *Int. J. Mod. Phys. D* **9**, 373 (2000); V. Sahni, *Lect. Notes Phys.* **653**, 141 (2004) [arXiv:astro-ph/0403324]; S. M. Carroll, *Living Rev. Rel.* **4**, 1 (2001); T. Padmanabhan, *Phys. Rept.* **380**, 235 (2003); P. J. E. Peebles and B. Ratra, *Rev. Mod. Phys.* **75**, 559 (2003); V. Sahni and A. Starobinsky, *Int. J. Mod. Phys. D* **15** 2105 (2006); S. Nojiri and S. D. Odintsov, *Int. J. Geom. Meth. Mod. Phys.* **4**, 115 (2007).
- [6] E. J. Copeland, M. Sami and S. Tsujikawa, *Int. J. Mod. Phys. D* **15**, 1753 (2006).
- [7] A. Melchiorri, L. Mersini-Houghton, C. J. Odman and M. Trodden, *Phys. Rev. D* **68**, 043509 (2003); J. Weller and A. M. Lewis, *Mon. Not. Roy. Astron. Soc.* **346**, 987 (2003); B. A. Bassett, P. S. Corasaniti and M. Kunz, *Astrophys. J.* **617**, L1 (2004); U. Seljak, A. Slosar and P. McDonald, *JCAP* **0610**, 014 (2006).
- [8] U. Alam, V. Sahni, T. D. Saini and A. A. Starobinsky, *Mon. Not. Roy. Astron. Soc.* **354**, 275 (2004); R. Lazkoz, S. Nesseris and L. Perivolaropoulos, *JCAP* **0511**, 010 (2005); J. Q. Xia, G. B. Zhao, B. Feng, H. Li and X. Zhang, *Phys. Rev. D* **73**, 063521 (2006); S. Nesseris and L. Perivolaropoulos, *JCAP* **0701**, 018 (2007); U. Alam, V. Sahni and A. A. Starobinsky, *JCAP* **0702**, 011 (2007); G. B. Zhao, J. Q. Xia, B. Feng and X. Zhang, arXiv:astro-ph/0603621.
- [9] R. R. Caldwell, *Phys. Lett. B* **545**, 23 (2002); R. R. Caldwell, M. Kamionkowski and N. N. Weinberg, *Phys. Rev. Lett.* **91**, 071301 (2003).
- [10] S. M. Carroll, M. Hoffman and M. Trodden, *Phys. Rev. D* **68**, 023509 (2003).
- [11] P. Singh, M. Sami and N. Dadhich, *Phys. Rev. D* **68** 023522 (2003); S. Nojiri and S. D. Odintsov, *Phys. Lett. B* **562**, 147 (2003); *Phys. Lett. B* **565**, 1 (2003); J. G. Hao and X. Z. Li, *Phys. Rev. D* **67**, 107303 (2003); P. F. Gonzalez-Diaz, *Phys. Rev. D* **68**, 021303 (2003); L. P. Chimento and R. Lazkoz, *Phys. Rev. Lett.* **91**, 211301 (2003); M. P. Dabrowski,

- T. Stachowiak and M. Szydlowski, *Phys. Rev. D* **68**, 103519 (2003); L. P. Chimento and R. Lazkoz, *Phys. Rev. Lett.* **91**, 211301 (2003); S. Tsujikawa, *Class. Quant. Grav.* **20**, 1991 (2003); M. Sami and A. Toporensky, *Mod. Phys. Lett. A* **19**, 1509 (2004); E. Elizalde, S. Nojiri and S. D. Odintsov, *Phys. Rev. D* **70**, 043539 (2004); H. Stefancic, *Phys. Lett. B* **586**, 5 (2004); V. B. Johri, *Phys. Rev. D* **70**, 041303 (2004); Z. K. Guo, Y. S. Piao and Y. Z. Zhang, *Phys. Lett. B* **594**, 247 (2004); J. M. Aguirregabiria, L. P. Chimento and R. Lazkoz, *Phys. Rev. D* **70**, 023509 (2004); S. Nojiri, S. D. Odintsov and S. Tsujikawa, *Phys. Rev. D* **71**, 063004 (2005); S. Nojiri and S. D. Odintsov, *Phys. Rev. D* **72**, 023003 (2005); L. Perivolaropoulos, *Phys. Rev. D* **71**, 063503 (2005); T. Chiba, *JCAP* **0503**, 008 (2005); M. Bouhmadi-Lopez and J. A. Jimenez Madrid, *JCAP* **0505**, 005 (2005); V. Faraoni, *Class. Quant. Grav.* **22**, 3235 (2005); L. P. Chimento, *Phys. Lett. B* **633**, 9 (2006); L. P. Chimento and D. Pavon, *Phys. Rev. D* **73**, 063511 (2006); O. Hrycyna and M. Szydlowski, arXiv:0704.1651 [hep-th].
- [12] A. Vikman, *Phys. Rev. D* **71**, 023515 (2005); Z. K. Guo, Y. S. Piao, X. M. Zhang and Y. Z. Zhang, *Phys. Lett. B* **608**, 177 (2005); W. Hu, *Phys. Rev. D* **71**, 047301 (2005); R. R. Caldwell and M. Doran, *Phys. Rev. D* **72**, 043527 (2005); H. Wei, R. G. Cai and D. F. Zeng, *Class. Quant. Grav.* **22**, 3189 (2005); G. B. Zhao, J. Q. Xia, M. Li, B. Feng and X. Zhang, *Phys. Rev. D* **72**, 123515 (2005); S. Tsujikawa, *Phys. Rev. D* **72**, 083512 (2005); I. Y. Aref'eva, A. S. Koshelev and S. Y. Vernov, *Phys. Rev. D* **72**, 064017 (2005); B. McInnes, *Nucl. Phys. B* **718**, 55 (2005); L. P. Chimento, R. Lazkoz, R. Maartens and I. Quiros, *JCAP* **0609**, 004 (2006); R. Lazkoz and G. Leon, *Phys. Lett. B* **638**, 303 (2006); X. F. Zhang and T. Qiu, *Phys. Lett. B* **642**, 187 (2006); W. Zhao, *Phys. Rev. D* **73**, 123509 (2006); H. Mohseni Sadjadi and M. Alimohammadi, *Phys. Rev. D* **74**, 043506 (2006); Z. K. Guo, Y. S. Piao, X. Zhang and Y. Z. Zhang, *Phys. Rev. D* **74**, 127304 (2006); I. Y. Aref'eva and A. S. Koshelev, *JHEP* **0702**, 041 (2007); Y. f. Cai, M. z. Li, J. X. Lu, Y. S. Piao, T. t. Qiu and X. m. Zhang, arXiv:hep-th/0701016; Y. F. Cai, T. Qiu, Y. S. Piao, M. Li and X. Zhang, arXiv:0704.1090 [gr-qc].
- [13] J. M. Cline, S. Jeon and G. D. Moore, *Phys. Rev. D* **70**, 043543 (2004).
- [14] N. Arkani-Hamed, H. C. Cheng, M. A. Luty and S. Mukohyama, *JHEP* **0405**, 074 (2004).
- [15] F. Piazza and S. Tsujikawa, *JCAP* **0407**, 004 (2004).
- [16] R. V. Buniy and S. D. H. Hsu, *Phys. Lett. B* **632**, 543 (2006).
- [17] S. Dubovsky, T. Gregoire, A. Nicolis and R. Rattazzi, *JHEP* **0603**, 025 (2006).
- [18] J. P. Uzan, *Phys. Rev. D* **59**, 123510 (1999); L. Amendola, *Phys. Rev. D* **60**, 043501 (1999); T. Chiba, *Phys. Rev. D* **60**, 083508 (1999); N. Bartolo and M. Pietroni, *Phys. Rev. D* **61**, 023518 (2000); F. Perrotta, C. Baccigalupi and S. Matarrese, *Phys. Rev. D* **61**, 023507 (2000); A. Riazuelo and J. P. Uzan, *Phys. Rev. D* **66**, 023525 (2002); D. F. Torres, *Phys. Rev. D* **66**, 043522 (2002); L. Perivolaropoulos, *JCAP* **0510**, 001 (2005); M. X. Luo and Q. P. Su, *Phys. Lett. B* **626**, 7 (2005); J. Martin, C. Schimd and J. P. Uzan, *Phys. Rev. Lett.* **96**, 061303 (2006).
- [19] B. Boisseau, G. Esposito-Farese, D. Polarski and A. A. Starobinsky, *Phys. Rev. Lett.* **85**, 2236 (2000).
- [20] R. Gannouji, D. Polarski, A. Ranquet and A. A. Starobinsky, *JCAP* **0609**, 016 (2006).
- [21] S. Capozziello, V. F. Cardone, S. Carloni and A. Troisi, *Int. J. Mod. Phys. D* **12**, 1969 (2003); S. M. Carroll, V. Duvvuri, M. Trodden and M. S. Turner, *Phys. Rev. D* **70**, 043528 (2004).
- [22] S. Nojiri, S. D. Odintsov and M. Sasaki, *Phys. Rev. D* **71**, 123509 (2005); M. Sami, A. Toporensky, P. V. Tretjakov and S. Tsujikawa, *Phys. Lett. B* **619**, 193 (2005); G. Calcagni, S. Tsujikawa and M. Sami, *Class. Quant. Grav.* **22**, 3977 (2005); B. M. N. Carter and I. P. Neupane, *JCAP* **0606**, 004 (2006).
- [23] L. Amendola, R. Gannouji, D. Polarski and S. Tsujikawa, *Phys. Rev. D* **75**, 083504 (2007). See also L. Amendola, D. Polarski and S. Tsujikawa, *Phys. Rev. Lett.* **98**, 131302 (2007); arXiv:astro-ph/0605384.
- [24] T. Koivisto and D. F. Mota, *Phys. Lett. B* **644**, 104 (2007); S. Tsujikawa and M. Sami, *JCAP* **0701**, 006 (2007); T. Koivisto and D. F. Mota, *Phys. Rev. D* **75**, 023518 (2007); B. M. Leith and I. P. Neupane, arXiv:hep-th/0702002.
- [25] L. Amendola, C. Charmousis and S. C. Davis, *JCAP* **0612**, 020 (2006).
- [26] A. De Felice, M. Hindmarsh and M. Trodden, *JCAP* **0608**, 005 (2006); G. Calcagni, B. de Carlos and A. De Felice, *Nucl. Phys. B* **752**, 404 (2006); Z. K. Guo, N. Ohta and S. Tsujikawa, *Phys. Rev. D* **75**, 023520 (2007).
- [27] G. R. Dvali, G. Gabadadze and M. Porrati, *Phys. Lett. B* **485**, 208 (2000).
- [28] G. Kofinas, R. Maartens and E. Papantonopoulos, *JHEP* **0310** (2003) 066 [arXiv:hep-th/0307138].
- [29] V. Sahni and Y. Shtanov, *JCAP* **0311**, 014 (2003).
- [30] A. Lue and G. D. Starkman, *Phys. Rev. D* **70**, 101501 (2004).
- [31] D. Gorbunov, K. Koyama and S. Sibiryakov, *Phys. Rev. D* **73**, 044016 (2006).
- [32] L. Senatore, *Phys. Rev. D* **71**, 043512 (2005); P. Creminelli, M. A. Luty, A. Nicolis and L. Senatore, *JHEP* **0612**, 080 (2006).
- [33] V. A. Rubakov, *Theor. Math. Phys.* **149**, 1651 (2006) [arXiv:hep-th/0604153].
- [34] B. M. Gripaios, *JHEP* **0410**, 069 (2004).
- [35] M. V. Libanov and V. A. Rubakov, *JHEP* **0508**, 001 (2005).
- [36] S. M. Carroll and E. A. Lim, *Phys. Rev. D* **70**, 123525 (2004).
- [37] J. P. Uzan, *Rev. Mod. Phys.* **75**, 403 (2003).
- [38] E. J. Copeland, A. R. Liddle and D. Wands, *Phys. Rev. D* **57**, 4686 (1998).
- [39] B. Gumjudpai, T. Naskar, M. Sami and S. Tsujikawa, *JCAP* **0506**, 007 (2005).
- [40] S. L. Dubovsky, *JHEP* **0410**, 076 (2004).
- [41] B. A. Bassett, S. Tsujikawa and D. Wands, *Rev. Mod. Phys.* **78**, 537 (2006).
- [42] J. M. Cline and L. Valcarcel, *JHEP* **0403**, 032 (2004); N. Arkani-Hamed, H. C. Cheng, M. Luty and J. Thaler, *JHEP* **0507**, 029 (2005); M. V. Libanov and V. A. Rubakov, *JCAP* **0509**, 005 (2005); *Phys. Rev. D* **72**, 123503 (2005); S. M. Carroll and J. Shu, *Phys. Rev. D* **73**, 103515 (2006); H. C. Cheng, M. A. Luty, S. Mukohyama and J. Thaler, *JHEP* **0605**, 076 (2006); S. Kanno and J. Soda, *Phys. Rev. D* **74**, 063505 (2006); P. G. Ferreira, B. M. Gripaios, R. Saffari and T. G. Zlosnik,

Phys. Rev. D **75**, 044014 (2007).

[43] M. Baldi, F. Finelli and S. Matarrese, Phys. Rev. D **72**, 083504 (2005).